
“COMPARISON OF DIAGNOSTIC ROLE OF DIFFUSION WEIGHTED
IMAGING IN THE DIFFERENTIATION OF BENIGN AND MALIGNANT
CERVICAL GROUP OF LYMPH NODES WITH PATHOLOGICAL
CORRELATION- A ONE YEAR OBSERVATIONAL STUDY AT KLES DR
PRABHAKAR KORE HOSPITAL AND MRC, BELAGAVI”

By
REGISTRATION NO. BS0118004

Dissertation

Submitted to the
KLE Academy of Higher Education and Research, Belagavi,
Karnataka

In partial fulfillment
of the requirements for the degree of

M.D.
IN
RADIO-DIAGNOSIS

DEPARTMENT OF RADIO-DIAGNOSIS,
J. N. MEDICAL COLLEGE,
BELAGAVI -590010. KARNATAKA

APRIL 2021

**KLE ACADEMY OF HIGHER EDUCATION AND RESEARCH,
BELAGAVI, KARNATAKA**

**Endorsement by the HOD/Principal/ Head of the
Institution**

This is to certify that the dissertation "COMPARISON OF DIAGNOSTIC ROLE OF DIFFUSION WEIGHTED IMAGING IN THE DIFFERENTIATION OF BENIGN AND MALIGNANT CERVICAL GROUP OF LYMPH NODES WITH PATHOLOGICAL CORRELATION- A ONE YEAR OBSERVATIONAL STUDY AT KLES DR PRABHAKAR KORE HOSPITAL AND MRC, BELAGAVI" is a bonafide research work done by REGISTRATION NO. BS0118004.

Dr. ASHWIN S PATIL
M.D. RADIO-DIAGNOSIS
Professor and Head,
Department of Radio Diagnosis,
J. N. Medical College,
Nehru Nagar, Belagavi – 10

Date:
Place: Belagavi

Dr. N.S. MAHANTASHETTI
M. D. PEDIATRICS
Principal,
J. N. Medical College,
Nehru Nagar, Belagavi – 10

Date:
Place: Belagavi

PALGIARISM CERTIFICATE



JAWAHARLAL NEHRU MEDICAL COLLEGE

(Recognized by Medical Council of India, New Delhi)

Accredited 'A' Grade by NAAC (2nd Cycle)

Placed in Category 'A' by MHRD (GoI)



Nehru Nagar, Belagavi- 590 010, Karnataka, INDIA

☎ 0831 - 2471350

☎ 0831 - 2470759

🌐 www.jnmc.edu

✉ principal@jnmc.edu

Ref No: MDC/PG/

Date: 21-10-2020

ACCEPTANCE LETTER

The softcopy of thesis entitled: "COMPARISON OF DIAGNOSTIC ROLE OF DIFFUSION WEIGHTED IMAGING IN THE DIFFERENTIATION OF BENIGN AND MALIGNANT CERVICAL GROUP OF LYMPH NODES WITH PATHOLOGICAL CORRELATION- A ONE YEAR OBSERVATIONAL STUDY AT KLES DR PRABHAKAR KORE HOSPITAL AND MRC, BELAGAVI" has been submitted for Anti-Plagiarism check through Turnitin software. The scan has been carried out and the scanned output reveals a match percentage of 5% which is within the acceptable limits of 10% as per the guidelines given by UGC.

Guide.




Chairperson-Antiplagiarism Committee &
Principal,
J. N. Medical College, Belagavi.

To,
Reg. No. **BS0118004**,
Postgraduate Student,
2018-19 Batch,
Department of Radiodiagnosis,
J. N. Medical College, Belagavi.

Abbreviations

Glossary	Abbreviations
ADC	Apparent diffusion coefficient
AIDS	Acquired Immuno-deficiency disease
CI	Confidence Interval
CT	Computed tomography
DWI	Diffusion Weighted Imaging
FDG	Fluoro-deoxyglucose
FNAC	Fine needle aspiration cytology
HNSCC	Head and neck Squamous Cell Carcinoma
HPR	Histopathological result
ICA	Internal Carotid Artery
IJV	Internal jugular vein
L/S ratio	Long axis / Short axis
LN _s	Lymph nodes
MRI	Magenetic resonance imaging
NPV	Negative predictive value
Par G	Parotid gland
PPV	Positive predictive value
ROC	Receiver operating characteristic
SAN	Spinal Accessory nerve
SCC	Squamous cell carcinoma
SCM	Sternocleidomastoid muscle
SD	Standard deviation
Sub G	Submandibular gland
TB	Tuberculosis
T1WI	T1 weighted image
T2WI	T2 weighted image
USG	Ultrasound

ABSTRACT

Background & objectives

“Lymphadenopathy” is defined as an abnormality in size and / or alteration in consistency of the lymph nodes. There are around 800 lymph nodes in the entire human body out of which 300 are present in the head and neck region. Common causes of the cervical lymphadenopathy are infection, metastasis from the neck primaries, granulomatous diseases and miscellaneous conditions like Castleman’s disease, Kikuchi’s disease, Kimura’s disease, Immunoblastic lymphadenopathy and post radiation changes. Most common infection resulting in cervical lymphadenopathy is tuberculosis in India. Most common metastases to the cervical nodes are seen in cases of carcinomas of oral cavity, tongue, larynx and pharynx.

Overall 57.8% of head and neck cancers occur in Asian continent, with a major bulk of cases seen in India. Out of these, 90% of the head and neck carcinomas are seen to arise from the mucosa of oral cavity and are of squamous cell origin.

Ultrasound, computed tomography and magnetic resonance imaging are the preliminary radiological modalities commonly used to diagnose the cases and plan the further management of the patients presenting with cervical lymphadenopathy. Nuclear studies like the Positron emission tomography (PET) and single photon emission CT (SPECT) are also included invariably but lack spatial resolution and may show false positive results due to high FDG take –up in the inflammatory nodes. MRI helps in characterizing the lymph nodes depending on the alteration in signal intensities on T1, T2 and DWI sequences and the Apparent Diffusion Coefficient (ADC) values involving the pathological lymph node. DW- MRI is an emerging, non-invasive modality in the detection of the nodes. It is mainly based on the principle of “Brownian motion” of the water molecules across the cell membranes and shows

diffusion restriction in the tissues with high cellularity. It helps in detection of metastasis in subcentimetric nodes in a substantial percentage of neck malignancies which are clinically inevident.

The aim of the study was to differentiate the cervical lymphadenopathy into benign and malignant etiology depending on the DW-MR imaging features and ADC values. The objective was to compare the findings of DWI/ ADC of cervical nodes to that of FNAC/ histopathology reports.

Materials and methods

One year prospective observational study was done in Department of Radiodiagnosis at the KLE'S Dr. PrabhakarKore hospital & MRC, Belagavi.49 patients clinically presenting with cervical lymphadenopathy were subjected to the MRI of neck after taking the written consent and considering the inclusion and exclusion criterias for characterization of the nodes and further management of the patients.

The sensitivity, specificity, positive predictive value, negative predictive values and accuracy of DWI of neck nodes was calculated and then compared with the pathological reports. For the continuous quantitative variables- mean and standard deviation were calculated. The threshold cut-off value for the differentiation of the nodes was obtained by plotting the Receiver operating Characteristic (ROC) curve.

Results

In this study, diffusion restriction was seen in 81.82% of the malignant nodes and 77.78% of the benign nodes did not show restriction of DWI with a significant “p” value of 0.0001. ADC values proved to be effective in characterizing the nodes into benign and malignant etiology with a sensitivity of 59.90%, specificity of 92.59%, positive predictive value of 86.6%, negative predictive value of 73.53% and an accuracy of 77.55% when compared to the pathological diagnosis. The ROC curve

was plotted to calculate the ADC threshold with an area of 0.7170 under consideration and was found to be $1.023 \times 10^{-3} \text{ mm}^2/\text{sec}$.

The mean ADC of benign nodes was $1.145 \times 10^{-3} \text{ mm}^2/\text{sec}$ and a standard deviation of 109.1, that of malignant nodes was $1.116 \times 10^{-3} \text{ mm}^2/\text{sec}$ and a standard deviation of 506.3. Out of the 22 malignant nodes, 4 nodes had central necrosis and hence showed high values suggesting the false negatives in the results obtained through ADC. The mean for the malignant nodes excluding the necrotic nodes was $0.972 \times 10^{-3} \text{ mm}^2/\text{sec}$. The mean ADC of reactive lymphadenitis was $1.094 \times 10^{-3} \text{ mm}^2/\text{sec}$. One of the nodes showed Non-Hodgkin lymphoma with significantly low ADC value of $0.550 \times 10^{-3} \text{ mm}^2/\text{sec}$.

The other variables which contributed to the diagnosis were – size of the nodes, shape, margins, status of fatty hilum, necrotic changes and the short axis dimension. The morphologic features on MRI like oval shape, well circumscribed margins, subcentimetric node, maintained fatty hilum, less than 1.0 cm of largest short axial diameter, absence of necrosis, absent diffusion restriction on DWI and higher ADC values (more than $1.023 \times 10^{-3} \text{ mm}^2/\text{sec}$) are suggestive of benignity. Whereas round shape, ill-defined margins, enlarged node, altered hilum, > 1 cm of largest short axial diameter, presence of necrosis, diffusion restriction on DWI and ADC values less than $1.023 \times 10^{-3} \text{ mm}^2/\text{sec}$ are features of malignancy.

Interpretation and conclusion

Cervical lymphadenopathy is a common condition in Indian set-up secondary to either infections, metastatic deposits or lymphomatous infiltration. DWI is an excellent modality with the advantage of it being non invasive and with no risk of radiation exposure to characterize the nodes. Other imaging modalities which can be used are- USG, CT, PET and SPECT with disadvantages like radiation exposure, low

spatial resolution in nuclear imaging or the limited field of view in USG. DWI and ADC has a high sensitivity and specificity for characterizing the lymph nodes.

This study concluded that the MR-DWI is the best modality for characterizing even the subcentimetric nodes and is major advantage over invasive procedures like the FNAC/ histopathology diagnosis with a high sensitivity, specificity, NPV, PPV and accuracy of the ADC values. Moreover the ADC values are also useful in differentiating the nodes from benign, metastatic and lymphomatous etiologies.

Keywords

Cervical lymphadenopathy, DWI/ ADC, diffusion restriction

CONTENTS

SL. NO.	TOPIC	PAGE NO.
1.	INTRODUCTION	1-2
2.	OBJECTIVES	3
3.	REVIEW OF LITERATURE	4-23
4.	METHODOLOGY	24-26
5.	RESULTS	27-47
6.	DISCUSSION	48-56
7.	CONCLUSION	57-58
8.	SUMMARY	59
9.	BIBLIOGRAPHY	60-65
10.	ANNEXURES	
	ANNEXURE I – CONSENT FORM	66-70
	ANNEXURE II – ETHICAL CLEARANCE LETTER	71
	ANNEXURE III – PROFORMA	72-73
	ANNEXURE IV – FIGURES	74-88
	ANNEXURE V – KEY TO MASTER CHART	89
	ANNEXURE VI – MASTER CHART	90-91

LIST OF TABLES

TABLE NO.	PARTICULARS	PAGE NO
1	Causes of cervical lymphadenopathy	15
2	Site of primaries and the commonly involved metastatic nodes	17
3	Age wise distribution of patients	28
4	Categorization of the benign and malignant lymph nodes by age groups	29
5	Level of the largest node studied	30
6	Categorization of the largest node into benign and malignant	31
7	Comparison of final diagnosis (Benign and malignant) with mean long axis and short axis by 't test'	32
8	Comparison of final diagnosis (Benign and malignant) with mean L/S ratio by 't test'	33
9	Shape wise distribution of the LN	34
10	Comparison of the final diagnosis with shape of the nodes	35
11	Distribution of the nodes depending on the margins	36
12	Comparison of the final diagnosis with the margins of the nodes	37
13	Necrosis wise distribution of the LNs	38
14	Comparison of the final diagnosis with the necrotic changes in the nodes	39
15	Differentiation of the nodes depending on the status of the fatty hilum	40
16	Comparison of the final diagnosis with the status of fatty hilum of the nodes	41
17	Short axis wise distribution	42

18	Comparison of the final diagnosis with the largest short axis dimension of the nodes	43
19	Distribution of the nodes depending on the diffusion restriction on DWI	44
20	Comparison of the final diagnosis with the status of diffusion of the nodes on DWI sequence	45
21	Comparison of final diagnosis (Benign and malignant) with mean ADC value by “t test”	46
22	Sensitivity, specificity, PPV, NPV and Accuracy of ADC values in differentiation of the nodes into benign and malignant categories	46

LIST OF GRAPHS

GRAPH NO	PARTICULARS	PAGE NO
1	Pie chart depicting age wise distribution of patients	28
2	Bar chart depicting categorization of the benign and malignant lymph nodes by age groups	29
3	Bar chart showing level wise distribution of the lymph nodes	30
4	Bar chart depicting level wise distribution of the lymph nodes into benign and malignant categories	31
5	Bar chart showing comparison of final diagnosis (Benign and malignant) with mean long axis and short axis dimensions	32
6	Bar graph showing Benign and malignant lymph nodes categorization with mean L/S ratio	33
7	Pie chart showing the shape wise distribution of nodes	34
8	Bar graph depicting the shape wise distribution of nodes	35
9	Pie chart showing distribution of the nodes depending on the margins	36
10	Bar graph showing characterization of the nodes depending on the margins	37
11	Pie chart showing distribution of the nodes depending on the necrotic changes within the nodes	38
12	Bar graph showing categorization of the nodes on the basis of necrotic changes	39
13	Pie chart showing distribution of patients depending on the status of the fatty hilum of the nodes	40

14	Bar graph showing categorization of the nodes depending on the preservation or loss of fatty hilum of the nodes	41
15	Pie chart showing distribution of patients depending on the largest dimension of the short axis of the nodes	42
16	Pie chart showing categorization of the nodes depending on the largest short axis dimension of the nodes	43
17	Pie chart showing distribution of nodes depending on the presence or absence of the diffusion restriction seen on DWI in the nodes	44
18	Bar graph showing categorization of the nodes depending on the diffusion restriction on DWI sequence	45
19	Receiver operating characteristic (ROC) curve of the ADC values used for differentiating benign from malignant lymph nodes	47

LIST OF FIGURES

FIGURE NO.	PARTICULARS	PAGE NO
1	Structure and histology of lymph node	6
2	Structures of the neck with its lymphatic drainage	8
3	Axial sections of T2 weighted MRI showing the levels of nodes at the level of; A-submandibular gland and B- parotid gland (Sub G- Submandibular gland; Par G- Parotid gland).	14
4	Levels of lymph nodes in neck on T2 weighted MR image - sagittal section	14
5	Restricted diffusion of molecules within a tissue.	18
6	Free diffusion of molecules within a tissue.	18
7	Diagrammatic representation of the variations seen on ADC in neoplastic tissues after undergoing chemo or radiotherapy due to its adverse reactions on the tissues resulting in alteration of the morphologic characteristics.	21
8	Pictorial representation of case 1- reactive lymphadenitis	
8	Pictorial representation of case 2- Squamous cell carcinoma of tongue with metastasis to bilateral level Ib and bilateral level II	74
9	Pictorial representation of case 3- Non-Hodgkin Lymphoma	75
10	Pictorial representation of case 4- Squamous cell carcinoma of tongue with lymph node metastases to right level Ib and right level III with necrotic components and extracapsular extension	77
11	Pictorial representation of case 5- K/C/O carcinoma of right buccal mucosa with 3 right level Ib lymph nodes shows metastases with extracapsular extension	79

12	Pictorial representation of case 6- Squamous cell carcinoma of tongue with metastasis to left level IIa node	82
13	Pictorial representation of case 7- Squamous cell carcinoma of tongue with no nodal metastasis	83
14	Pictorial representation of case 8- Mucoepidermoid carcinoma of left parotid gland with metastases to left level Ib and IIa lymph nodes	86

INTRODUCTION

Lymph is a derivative of interstitial fluid that flows into the lymphatics. The system of lymphatic flow is a major route for absorption of nutrients, proteins and also the bacteria from the interstitial tissue.

This systemic flow of lymph in the cervical region has 300 nodes out of the total of 800 nodes in the entire body.

Head and neck cancers have been represented to be the most common cancers worldwide. More than 90% of cervical region carcinomas are seen to arise from the mucosa of oral cavity and are of squamous cell histological type (HNSCC). Lymphatic spread to regional nodes is seen early in the progress of disease.¹ Overall, 57.5% cancers of neck structures occur in Asia, especially India.²

“Lymphadenopathy” is defined as an abnormality in size and / or alteration in consistency of the lymph nodes. It is proven to result from many conditions, including infections, autoimmune disorders or malignancies (metastatic or lymphomas). A meta-analysis by Dünne et al. showed a short term survival of 5-years between 17% and 55.8% for SCC with cervical node metastases and 44.6–76% for SCC patients without cervical node metastases. Detection of multiple metastatic lymph nodes (LNs) has bad prognosis.³

DWI is a non invasive procedure and it will allow for the noninvasive detection of metastases in normal-sized nodes in a substantial percentage of cases suspected which present with cervical regional masses or proven malignancies. It will characterize the lymph nodes in accordance with the morphologic criteria like size criteria, shape, irregular, illdefined border, discrete

or matted, presence of fatty hilum and/or symmetric localization of lymph nodal involvement depending on the signal intensities on T1WI, T2WI, DWI sequences and the ADC values in the Region of Interest (ROI) drawn involving the pathological lymph node.⁴

Differentiation of the nodes is a necessity for oncologic staging. It will not only affect the therapeutic plan but also improve patient's prognosis.

This study mainly focuses on detecting the malignant or metastatic lymph nodes in patients without going for discomforting invasive studies and without the risk of exposure to radiation.

AIM & OBJECTIVES

AIM

1. To differentiate the cervical adenopathy into that of benign etiology and malignancy depending on the DW-MR imaging features and ADC values.

OBJECTIVE

1. To compare the findings of DWI/ADC of cervical nodes to that of FNAC/histopathological reports.

REVIEW OF LITERATURE

HISTORICAL REVIEW OF THE ANATOMY OF LYMPH

Herophilos 300 B.C, one of the members of the Alexandrian school, first described the lymphatic anatomy in 1062. GasparoAselli, head of surgery department in Milan, described the lymphatic vasculature in the dog's mesentery. Kean in 1651 (from France) described the receptaculumChyliand thoracic duct. The term "lymphatic" was first coined in 1653 by Thomas Bartholin.⁵

Upto 17th century, there was limited information available regarding the anatomic and pathophysiologic study of the flow of lymph in human and animal body. Frederik R Ruysch (from the year 1638 to 1731), a "praelectoranatomiae" of the Amsterdam Guild of Surgeons, was considered the pioneer in this field. He had a major role to play in contribution to the anatomic details in the form of lymphatic valves through anatomic dissection procedure.⁶

Rudolf Virchow, a well know pathologist from Germany, from the year 1821 to 1902 came to a conclusion that lymphatic structures function as filters to the flowing lymph and are the site for cancerous cells deposition which will lead to further spread of these rapidly multiplying cells to the other nodes.⁷ Donald Morton from 1934 to 2014 developed the technique of sentinel nodal biopsy which was of great help in staging the melanomas accurately and avoiding unnecessary nodal dissection.⁸ Subsequently, physicians and surgeons began to believe that local management of the carcinomashasto be supplemented with treatment of the regional lymphatic anatomical structuresto improvise the rate of cure. Hence, the nodal dissection on table became an essential element of oncology management.⁹

Lymphatic Embryology:

According to Sabin, lymphatic system originates from the aggregate of five primitive lymphatics which she originally called “lymph hearts”. Sabin stated that these sacs develop from venous system. In a two month gestational embryo of human being, these sacs are completed; giving rise to the paired jugular sacs along the corresponding vein, unpaired retroperitoneal sac at the mesenteric root and paired posterior sacs along the sciatic vein. Out budding of these sacs propagate centrifugally to form the peripheral system. The head and arms receive a plexus of lymphatics from jugular sacs. The mesentery receives the lymphatics from the retroperitoneal sacs.¹⁰

Secondary lymphatic structures develop shortly after the primary system and include cisterna chyli, thoracic duct and subclavian lymph sacs. Formation of all the sacs is completed by eighth week of gestation.

A well known French scientist, Jean Pecquet, succeeded in demonstrating that chyle produced from the abdominal organs passes through the cistern chyli and the lymphatic duct in the thorax called the thoracic duct which further flows to the right subclavian vein.^{11, 12}

Next, Thomas S. Bartholin and O. Rudbeck proposed in their theory that the lymph flows from the liver into the thoracic cavity and also forms a widespread network in the entire body draining the regional organs. They also named these vessels as “vasa lymphaticae” which was later modernized to the recent terminology of lymphatic vessels by Thomas Bartholin.^{13, 14}

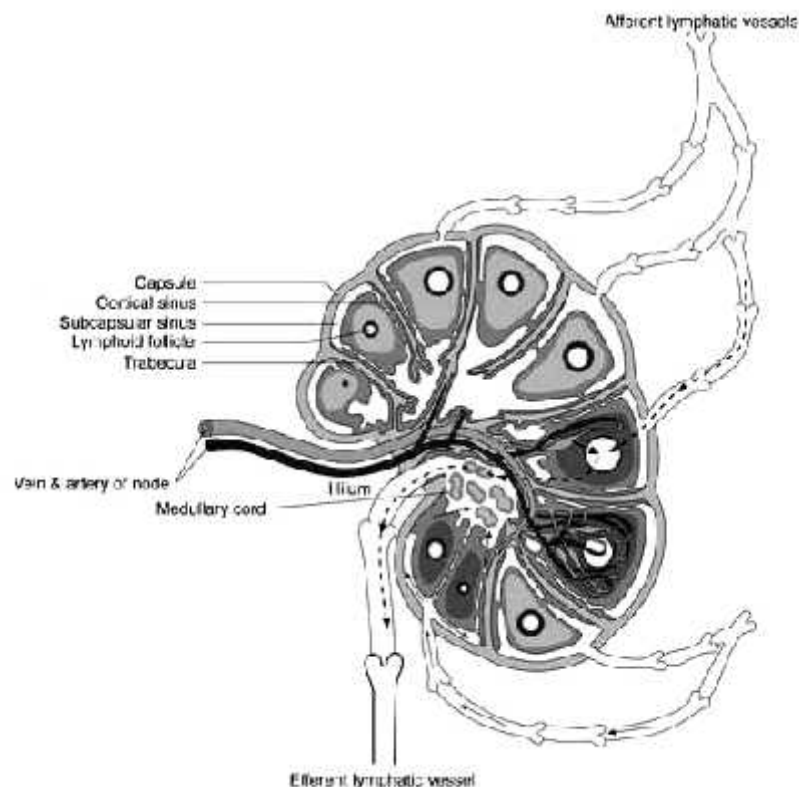
According to theory proposed by William Hunter in the 18th century, these vessels containing lymph are perceived to be absorbing vessels distributed in all the

regions of the body. He termed these vessels as the “absorbent system”.¹⁵ William Hewson, a pupil of William Hunter, made extensive dissections of the system, in the aquarian fishes and mammals.¹⁵ He gave the theory stating that, there appears a cyclical rhythmic contraction in these vessels and the presence of multiple valves within it to prevent the retrograde flow of lymph.

In the year 1869, Arnold Heller gave the theory of intrinsic phasic contractions within the lymphatic vessels in the mesentery of the guinea pig and termed it as lymphatic retropulsion.¹⁶

ANATOMY¹⁷

Figure 1: Structure and histology of lymph node



The nodes in the neck region are small bean shaped structures. A noticeable depression is seen in the midline on one side termed hilus, from where the blood vasculature enter (afferent) and leave the node (efferent). It has an outer cortex, middle paracortex and inner medulla. The cortex is deficient at the hilus. The efferent vessels directly originate from the inner medulla while the afferent vessels have a drainage into the outer cortex.¹⁷

The capsule, made up of “collagen fibers” and some “elastic fibers”, forms the external cover. The paracortex acts as a transitional area for the lymphocytes to reach back to its parent system from the vascular anatomy. Lymphoid follicles form the cortex. The central medulla contains the trabeculae, cords and the sinuses.

Arterial System:

The main artery enters at the hilum and divides into further branches. In the outer cortical portion, the arterioles further branch into capillaries to terminate into lymphoid follicles. In the central medullary region, few arterioles run along the trabeculae up to the cortex whereas some end up supplying the capillaries.¹⁷

Venous System:

Venous and the arterial systems follow a similar route through the hilus. In the cortex, number of venules converge and form a small vein which further converges and give rise to the main vein in medulla. The main draining vein exits through the hilus.^{5,17}

ipsilateral chain, except the midline structures- that includes the laryngeal, nasopharyngeal & pharyngeal structures and tongue base. They are classified as Ia, Ib, IIa, IIb, III, IVa, IVb, Va, Vb, Vc, VIa, VIb, VIIa, VIIb, VIII, IX, Xa and Xb.¹⁸

The boundaries of the LNs are defined in reference to the patient lying in supine position with his/her head in a “neutral” position.

Level I

Level Ia is located in the midline between anterior bellies of bilateral digastrics, called the submental nodes. They drain the skin over the chin, the mid part of inferior lip, anterior aspect of floor of mouth and tongue (only the tip). Hence are most vulnerable to metastases from primaries of these locations.

Ib are submandibular group of nodes. Lateral boundary is the mandible bone and medial is the digastric. The space extends from symphysis menti reaching up to the submandibular salivary glands. They receive flow from nasal cavity (lower aspect) and both hard & soft palate, two alveolar ridges (upper maxillary and lower mandibular), cheek region and anterior 2/3rd of tongue. These nodes have metastases from primaries of nasal & oral cavity, mid-face & salivary glands of submandibular space.

Level II, III and IV

These are called the upper, mid and lower jugular nodes forming a chain along the superior, middle and inferior 1/3rd of the XIth cranial nerve (SAN) and IJV. Their lateral extent is up to SCM and medial extent up to scalenus muscle and medial margin of ICA. Upper 1/3rd of jugular group is seen to extend from the first cervical vertebra to hyoid. Middle jugular from inferior margin of upper jugular group to the cricoid ring cartilage & the lower ones extend up to an arbitrary line drawn 2 cm above

the joint formed by sternum and clavicle. Jugular vein divides the “II group” of nodes into IIa&IIb. Level II receives lymph draining from the subcutaneous and muscular plane of face, retropharyngeal nodes and the three pairs of salivary glands (major glands), nose, pharyngeal & laryngeal tissues, middle ear & external ear meatus, and hence harbour secondaries from these primaries. Mid jugular, retropharyngeal, Waldeyer ring system, base of tongue and thyroid glands drain into middle jugular nodes.

Level IVa and IVb are subdivided by SCM. They have secondary deposits from epicentres which include laryngo-pharyngeal tissue, thyroid gland, nasopharynx, and pharyngeal tonsils. IVb are the medial supraclavicular nodes.

Level V (Va, Vb and Vc)

Va and Vb group are located in the posterior triangle demarcated by the cricoid cartilaginous structure for oncologic dissections. Vc are lateral supraclavicular nodes. Anterior boundary being the transverse cervical vasculature & SCM and posterior being trapezius. Superior extent is a plane that passes along the superior margin of mid portion of hyoid and inferior extent is the cervical transverse artery. Lateral limits extend upto the epidermis and underlying superficial platysma muscle. Medial extent is the muscle of back (levator scapulae) cranially and posterior scalenus caudally.

Level Va and Vb are seen to drain the posterior scalp region (parieto-occipital regions), the skin over the shoulders and naso& oropharynx. These should be looked with great degree of suspicion in case of primaries of midline anatomic structures like the thyroid & pharynx.

Level Vc

They are called the lateral group of supraclavicular nodes which share common boundary with level IVa, inferior margin of level IVa marks the superior extent of Vc. Anterior extent reaching up to the epidermis and postero-laterally the trapezius. Medially, reaching up to the lateral margin of SCM. Commonly involved in nasopharyngeal carcinomas.

Level VIa and VIb

VIa and IVb groups lie in between the bilateral SCMs and common carotid arteries respectively.

The first group comprises the anterior compartment nodes located in front of the airways in visceral space and shares a common boundary with level Ib nodes- superior extent of VIa is hyoid and inferior being glands located in submandibular space. The boundaries, anteriorly, being platysma & posteriorly, strap muscles. Nodal involvement must be suspected in cases of carcinomas of buccal mucosa of gingivo-mandibular sulcus and lips.

The second group rests on membrane joining the thyroid & hyoid and receives lymphatic flow from the tongue (tip), lip (lower) and structures below the mylohyoid muscle and thus are at risk of having metastatic deposits from these regions. Lower boundary is the manubrium of sternum and upper is the cartilaginous tissue covering the thyroid, medial is the trachea & esophagus and lateral is the common carotid on either sides. They receive efferents from the vocal cords and subglottis, adjacent pyriform sinuses, esophagus (cervical portion) and oral cavity structures.

Level VIIa and VIIb

These are the retropharyngeal and retro-styloid nodes respectively.

The first group lie in the retropharyngeal space extending from the atlas vertebrae to hyoid bone with lateral extension upto the internal carotids. Ventrally it extends upto the intrinsic pharyngeal musculature – the superior constrictor and dorsally upto the longus group of muscles. Their involvement should be suspected in neoplastic etiologies of the Waldeyer's ring tissues and internal auditory canal.

The second group is the proximal extension of II group nodes, situated in the carotid and prestyloid portion of parapharyngeal spaces with posterior extension being body of first vertebra of vertebral column and inferiorly upto the jugular foramen. They are vulnerable to the primaries of the nasopharynx and are proven to have retrograde flow from extensive level II involvement and thus should be noticed carefully with high grade of suspicion in cases with massive lesions of neck regions.

Level VIII

They are called the parotid group, comprising of the sub- and intraparotid nodes. They are suspended in the subcutaneous plane of pre-auricular region extending from lower margin of zygomatic bone upto the lower border of ramus of mandible. Anterior & posterior limits are the masticator space and digastric muscle respectively.

Their extensions are from subcutaneous plane laterally to styloid bone medially. Anteriorly from the pterygoid and masseter muscles, to the SCM & digastric

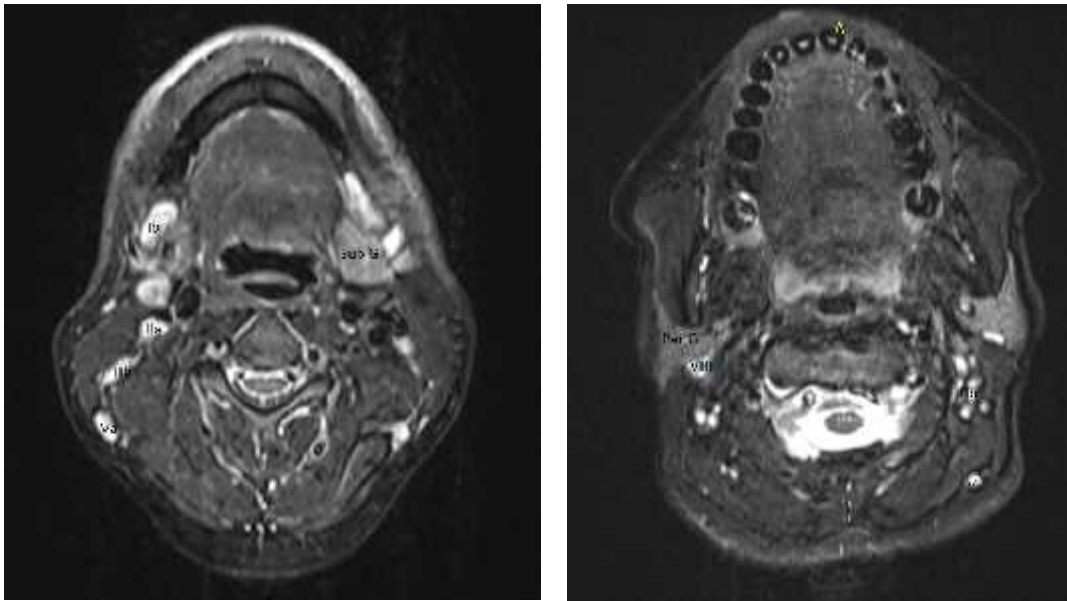
muscle (posterior belly) posteriorly. They have drainage areas from the pinna, nose, Eustachian tube, skin covering the eyes, temporal fossa and forehead.

Level IX

These are bucco-facial and malar groups, suspended in the subcutaneous plane of face and buccal fat pad covering the superficial face muscles like buccinators on its medial aspect and the masseter on the ventral aspect. They are mostly vulnerable to the primaries of face, nose, cheek and the maxillary air sinuses.

Level Xa and Xb

Xa are the retroauricular (also called mastoid) and subauricular groups that form a chain along the mastoid processes with extensions as mentioned below- plane passing along the external auditory meatus (superior margin) to inferior end of mastoid bone and anteriorly from the parotid space to the occiput posteriorly. These groups harbour the least metastases and are involved only in ear and occipital region primaries. Xb is the occipital group, with anterior boundary being the lateral most SCM and posterior being the trapezius muscle. Again these are involved in skin neoplasms of posterior occipital scalp region.¹⁸



A

B

Figure 3: Axial sections of T2 weighted MRI showing the levels of nodes at the level of; A- submandibular gland and B- parotid gland (Sub G- Submandibular gland; Par G- Parotid gland).



Figure 4: Levels of lymph nodes in neck on T2 weighted MRI image -sagittal section.

CERVICAL LYMPHADENOPATHY

Process of identifying and classifying the causes of lymphadenopathy in neck requires a meticulous approach. There are multiple conditions which present with cervical region lymphadenopathy, most commonly seen are the infectious causes and metastatic deposits.¹⁹

Table 1: CAUSES OF CERVICAL LYMPHADENOPATHY²⁰
<p><u>Infections</u></p> <p>Gram stain - negative and positive bacteria</p> <p>Tick borne disease- Borreliosis</p> <p>Cytomegalovirus infection</p> <p>Glandular fever/ kissing disease</p> <p>German measles</p> <p>Teeny's disease</p> <p>Toxoplasmosis</p> <p>AIDS</p>
<p><u>Granulomatous disease</u></p> <p>Typical /atypical mycobacterial infection</p> <p>Besnier-Boeck-Schaumann disease – sarcoid granulomas</p> <p>Hand-Schüller-Christian disease</p>
<p><u>Neoplasms</u></p> <p>Metastases from SCC of oropharynx, Thyroid Carcinoma (most commonly - Papillary Carcinoma of thyroid), lung, Esophagus, Renal carcinomas</p> <p>Non-Hodgkin's & Hodgkin's Lymphoma</p> <p>Kaposi sarcoma</p>
<p><u>Miscellaneous (rare)</u></p> <p>Castleman's or Kikuchi's or Kimura's disease</p> <p>Immunoblastic lymphadenopathy</p> <p>Histiocytoid hemangioma</p> <p>Post radiation changes</p>

INFECTIONS:

The common organisms include *Mycobacterium tuberculosis*, *Mycobacterium avium* complex, *Bartonella henselae*, Cytomegalovirus virus, Rubella and Epstein – Barr virus.

Tuberculosis lymphadenitis occurs as a local presentation of some underlying systemic disease. *Mycobacterium tuberculosis* is a gram positive organism that enters human body, in the form of aerosols, through the airway tract and undergoes haematogenous and lymphatic dissemination. Hilar and mediastinal LNs are the sentinel nodes to manifest morphologic changes secondary to pulmonary TB. Tonsil is also an important portal for the organism to multiply and propagate with the subsequent involvement of cervical LN.^{21,22}

The following groups are involved (in order of decreasing frequency): Anterior cervical, Posterior cervical, Supraclavicular, Submandibular, Submental and Preauricular. They are enlarged and matted with necrotic changes due to caseous necrosis. In later stages, tubercular abscess might be the sequelae.

In cases of reactive lymphadenitis, the LNs are oval shaped, well circumscribed with well preserved hilar fat. On DWI imaging, it does not show restriction.²³

METASTATIC CERVICAL LYMPHADENOPATHY

Large number of patients with head region carcinomas present with early metastasis to the regional nodes. Almost 58% worldwide cases occur predominantly in the Asian continent, especially India.² The lesions metastasize commonly to the

anterior triangle nodes with primaries in the buccal mucosa, tongue, laryngeal and pharyngeal structures.

Table 2: Site of primaries and the commonly involved metastatic nodes

PRIMARIES	COMMONLY INVOLVED NODES IN METASTASES
Oropharynx, hypopharynx, larynx carcinomas	Level II, III and IV
Oral cavity and tongue carcinomas	Level Ib and II
Papillary carcinoma of the Thyroid	Level II, III and IV
Nasopharyngeal carcinoma	Level II and V
Non-head and neck carcinoma	Level Va and Vb

IMAGING MODALITIES:

Ultrasound, computed tomography and magnetic resonance imaging are the preliminary radiological modalities commonly used to screen the patients to reach a diagnosis. The management of the cases is largely dependent on the radiological diagnosis in patients presenting with swelling in neck. Nuclear studies like the Positron emission tomography (PET) and single photon emission CT (SPECT) are also included invariably but lack spatial resolution and may show false positive results

due to high FDG take –up in the inflammatory nodes. Whereas pathological diagnosis like FNAC is operator dependant and moreover an invasive procedure.^{24,25}

DWI is an MRI based sequence that works on the principle of the tissue characterization depending on tissue microenvironment.^{24,25} The basic principle involved in DWI is the motion of water molecules across the membranes of cells. It is named as the “Brownian motion”. The analysis of the lesions is largely dependent on the water motion across the cell membranes as microstructural changes in tissues will result in alteration of the movement of molecules, thus resulting in altered signal intensities.^{26,27,28} The amount of restriction in a given biologic tissue is inversely related to the membrane intactness and tissue cellularity.^{29,30} The degree to which there is seen restriction of movement of molecules containing protons is directly proportional to the cellularity of the tumour containing tissues.^{31,32,33,34}

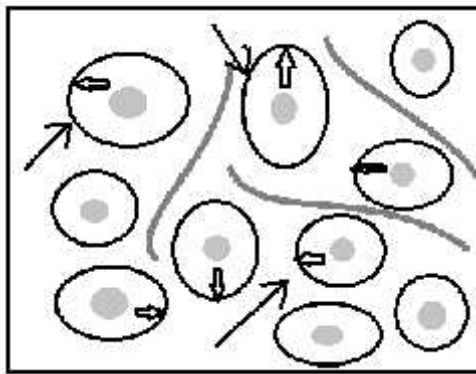


Figure 5: Restricted diffusion of molecules within

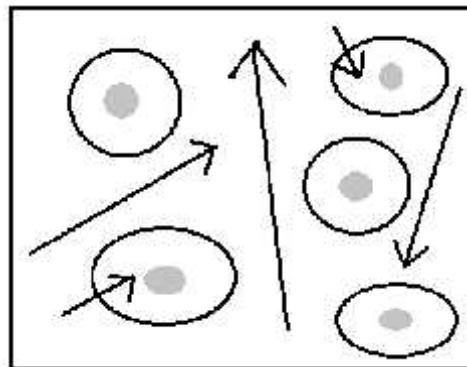


Figure 6: Free diffusion of molecules within a tissue

The sensitivity of detection on DWI sequence is dependent on three parameters- the ‘time duration’ for which the gradient is applied, the ‘amplitude of the gradient’ for that particular tissue and ‘interval of time’ for the area of interest for the applied pair of gradients. For clinical purposes, the sensitivity of detecting the minute anatomic alteration can be changed by applying different “values of b”, which is

subjective to the above mentioned parameters. The alteration in b value results in alteration in amplitude rather than altering the time factors. b values range from 0, 50, 500, 1000 and 2000 sec/mm². Higher b values can pick up signals from the short diffusion distances. A human cell measures 10 μm and the mean of root square displacement of diffusion is calculated to be 8 μm.³⁵ Hence DWI is proven as an excellent imaging modality to determine the microstructural changes in the cancerous tissue.

Isotropic ADC

$$D_I = \frac{D_x + D_y + D_z}{3}$$

D_I- isotropic ADC

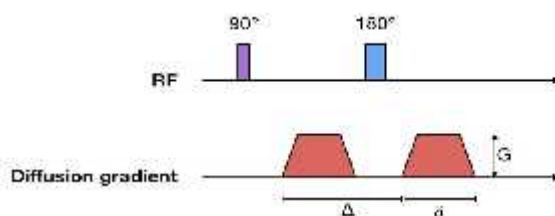
D_x- diffusion value calculated with gradients applied in x direction

D_y- diffusion value calculated with gradients applied in y direction

D_z- diffusion value calculated with gradients applied in z direction

b value

$$b = \gamma^2 G^2 \delta^2 \left(\Delta - \frac{\delta}{3} \right)$$



γ = gyromagnetic ratio

G = magnitude of the two balanced DW gradient pulses

δ = width of the two balanced DW gradient pulses

Δ = time between the two balanced DW gradient pulses

**Relationship between
signal of b = 0, DWI and ADC**

$$S_{DWI} = S_{b=0} \times e^{(-b \times D)}$$

equivalent to...

$$D = -\frac{1}{b} \times \ln\left(\frac{S_{DWI}}{S_{b=0}}\right)$$

S_{DWI} = signal intensity of isotropic DWI

$S_{b=0}$ = signal intensity of b = 0

b = b value

D = apparent diffusion coefficient (ADC)

The morphologic characteristics taken into consideration while imaging includes – size, shape, margins, maximum short axial diameter, long axis/ short axis ratio (L/S ratio), loss of fatty hilum, presence of cystic or necrotic changes, calcifications, pattern of contrast enhancement and perinodal infiltration.

DWI is a non invasive procedure and it will allow for the non-invasive detection of metastasis in subcentimetric nodes in a substantial percentage of cases with suspected neck masses or proven malignancies with metastatic lymphadenopathy to the LN that are clinically invident. MRI helps in characterizing the LN depending on the alteration in signal intensities on T1, T2 and DWI sequences and the Apparent Diffusion Coefficient(ADC) values involving the pathological lymph node. The characterization of the LNs helps in planning the further management in oncologic cases.

In neoplasms, post treatment with chemotherapy or post radiation, in the initial stages there is seen high intracellular water content resulting in cell

swelling.³⁶This reflects on ADC as low signal intensity. At a later stage, it results in death of the cell called necrosis which is depicted as high signal intensity on ADC. Later the cell goes into a process of autolysis due to autodigestion by the lysosomes and the enzymes released by them.^{37,38}

In few cases, there is seen apoptosis of cells post-treatment, which causes cell shrinkage and it is seen as high signal on ADC. These apoptotic cells later go for secondary lysis. When the entire treatment is over, there appears a phase of re-equilibrium wherein there is resorption of extracellular fluid which depicts as restriction. In case of recurrence or residual lesions there is seen diffusion restriction with low ADC in the tumour.^{39,40}

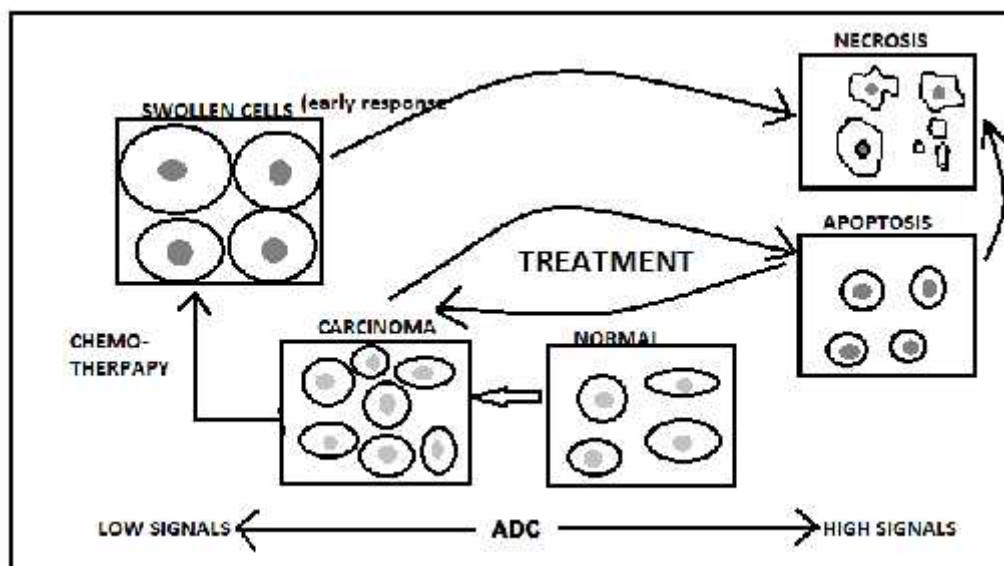


Figure 7: Diagrammatic representation of the variations seen on ADC in neoplastic tissues after undergoing chemo or radiotherapy due to its adverse reactions on the tissues resulting in alteration of the morphologic characteristics.

A study conducted at G.M.C. Patiala showed, out of 60 patients, 41 (68.33 %) cases came out as malignant and 19 (31.67 %) cases came out as benign. The results

derived were - 36 true positives, 4 false positives, 15 true negatives and 5 false negatives. The sensitivity of DWI for characterizing cervical lymphadenopathy was 87.80% with specificity of 78.95%. The PPV & NPV found were 90.00% and 75.00% respectively. The best ADC threshold value for distinguishing benign and malignant nodes was $1.005 \times 10^{-3} \text{ mm}^2/\text{sec}$.¹

A study conducted at Italy enrolled 32 subjects: 14 with benign lymphadenopathy, 17 patients with histologically proved malignant disease before beginning treatment and 01 patient of lymphoma after chemotherapeutic treatment. 13/14 patients having benign etiology in nodes presented with absent restriction on DWI and had corresponding high signals on ADC maps, whereas all patients showing malignant nodes showed diffusion restriction on DWI and reversion on ADC. One patient who was diagnosed with mycobacterium tuberculosis appeared hypointense on ADC. The mean value of ADC in benign cases was $1.448 \times 10^{-3} \text{ mm}^2/\text{s}$ and that of malignant was $0.85 \times 10^{-3} \text{ mm}^2/\text{s}$ with a threshold value of $1.03 \times 10^{-3} \text{ mm}^2/\text{s}$. The study showed a sensitivity & specificity of 100% and 92.9% respectively.⁴

Abish Y. G.et. al. conducted a study on 35 cases with suspected metastatic lymphadenopathy. The ADC for benign, malignant & lymphomatous etiology was $1.48 \pm 0.32 \times 10^{-3} \text{ mm}^2/\text{s}$, $0.91 \pm 0.73 \times 10^{-3} \text{ mm}^2/\text{s}$ and $0.75 \pm 0.04 \times 10^{-3} \text{ mm}^2/\text{s}$ respectively and $p < 0.0001$. The mean of metastatic nodal ADC was proven to be significantly lower than the lymphomatous nodes. Among the lymphomas, the Non-Hodgkin types were proven to have ADC values (mean ADC $0.64 \pm 0.86 \times 10^{-3} \text{ mm}^2/\text{s}$) significantly lower than that of Hodgkin type (mean ADC $0.85 \pm 0.91 \times 10^{-3} \text{ mm}^2/\text{s}$). And among the metastatic nodes, the ADC of moderately differentiated carcinomas

(mean of $0.97 \pm 0.94 \times 10^{-3} \text{ mm}^2/\text{s}$) were significantly more in comparison to the poorly differentiated ($0.82 \pm 0.56 \times 10^{-3} \text{ mm}^2/\text{s}$) ($p=0.03$); suggesting that poorly differentiated have more cellularity and thus are more infiltrative and aggressive tumours.⁴¹

A study conducted with a sample size of 34 patients with suspected cervical nodal enlargement showed nine inflammatory lymphadenopathy (lymphadenitis) cases, 11 lymphoma cases and 14 with metastases with a average ADC of $1.51 \pm 0.36 \times 10^{-3} \text{ mm}^2/\text{sec}$, $0.74 \pm 0.14 \times 10^{-3} \text{ mm}^2/\text{sec}$ and $0.92 \pm 0.13 \times 10^{-3} \text{ mm}^2/\text{sec}$ respectively, suggestive of decreasing values of ADC from benign etiology to metastatic and lymphomatous involvement.²¹

A study conducted at Cairo University, Egypt in 2014 included twenty six patients. 32 nodes were studied, out of which 24 nodes were malignant and 8 were benign. The results obtained were compared with the histopathology reports. DWI and ADC values of 27 malignant lesions (84%) & 5 benign (16%) were obtained and showed an accuracy of 89% of DWI helping in correctly characterizing the nodes. The statistical data analysis revealed 24 true-positives, 3 false-positives, 5 true-negative findings, yielding 100% sensitivity, 62.5% specificity%, NPV = 100% and PPV = 89%.⁴²

METHODOLOGY

Source of data: Patients referred to Radio-Diagnosis Department at The KLE'S Dr.Prabhakar Kore hospital & MRC, Belagavi to undergo MRI scan for suspected cervical lymphadenopathy or cervical region masses.

Study design: The current study was a prospective observational study.

Sample size: The sample size was calculated based on the current incidence of 57.5% of population in India presenting with mass lesions and malignant nodes in neck as quoted in a study done by Kulkarni M. R. in the article "Head and neck cancer burden in India". Considering percentage likely difference in the prevalence of 25%, a sample size of 45 was obtained. However final sample size analyzed in this study was 49.

Sampling method: All the eligible subjects were recruited into the study by convenient sampling till the sample size was reached.

Study duration: The data collection for the study was done from January 2019 to December 2019, for a period of 1 year.

Inclusion Criteria:

1. Age of patients ranging from 10 to 90 years, including pregnant women.
2. Patients with suspected or proven head and neck malignancies or benign etiologies.
3. Operated cases of head and neck malignancies with suspected metastasis in cervical lymph nodes.
4. Patients with clinically suspected cervical lymphadenopathy.

Exclusion criteria:

1. Patients with known contraindications to MRI.
2. Patients lost to follow-up.

Ethical considerations: Study was approved by the institutional human ethics committee. Informed written consent was obtained from all the study participants, and only those participants willing to sign the informed consent were included in the study. Confidentiality of the study participants was maintained.

Data collection tools: All the relevant parameters were documented in a structured study proforma.

Methodology:

After obtaining the informed written consent, all the study participants were evaluated with a thorough clinical history and physical examination of the swellings was done. Demographic details of the patient, chief complaints, past & family history of any malignancy and treatment history were collected.

The patients were subjected to MRI in 1.5 Tesla MRI scanner (Magnetom Avanto TIM, 18 channel; Siemens, Erlangen, Germany) and 3.0 Tesla MRI scanner (Magnetom Spectra, 32 channel; Siemens, Erlangen, Germany). And the sequences mainly obtained were axial, coronal and sagittal images of T1 & T2 spin echo sequences and DWI & ADC maps.

Statistical Methods:

Age, levels of LN involvement, size, short axial dimension, shape, margins, evaluation of fatty hilum, necrosis and diffusion restriction with ADC were the variables evaluated.

For the continuous quantitative variables-mean and standard deviation were calculated. For the purpose of comparison, the data was divided into two groups with respect to certain qualitative characteristics, the continuous variables were compared using suitable tools of statistics like unpaired student's 't' test. The study diagnosis was compared to the final diagnosis and the outcome was given using Chi-square test.

For all the tests the value of "p" less than 5% (0.05) was considered significant.

RESULTS

A total of 49 patients referred to the department of Radio-diagnosis for evaluation of the cervical lymphadenopathy with MRI were included ranging from 10 to 90 years of age. These patients were later followed up with their histopathological / FNAC results. On evaluation of the pathological reports, 27 turned out to be benign and 22 malignant. On DWI correlation, 24 (48.98%) showed diffusion restriction and 25 (51.02%) did not show restriction. Out of the 24 nodes which showed diffusion restriction, 18 (81.82%) were malignant and 6 (22.22%) were benign and out of 25 which did not show restriction, 21 (77.78%) were benign and 4 (18.18%) were malignant. This study proved to be significant with a “p value” of 0.0001. The in detail results of the other variables taken into consideration for characterization of nodes is tabulated below.

Table 3: Age wise distribution of patients

Age groups	Number	Percentage
<=40yrs	9	18.37
41-50yrs	9	18.37
51-60yrs	12	24.49
61-70yrs	10	20.41
>=71yrs	9	18.37
Total	49	100.00
Mean age	54.78	
SD age	17.98	

Graph 1: Pie chart depicting age wise distribution of patients

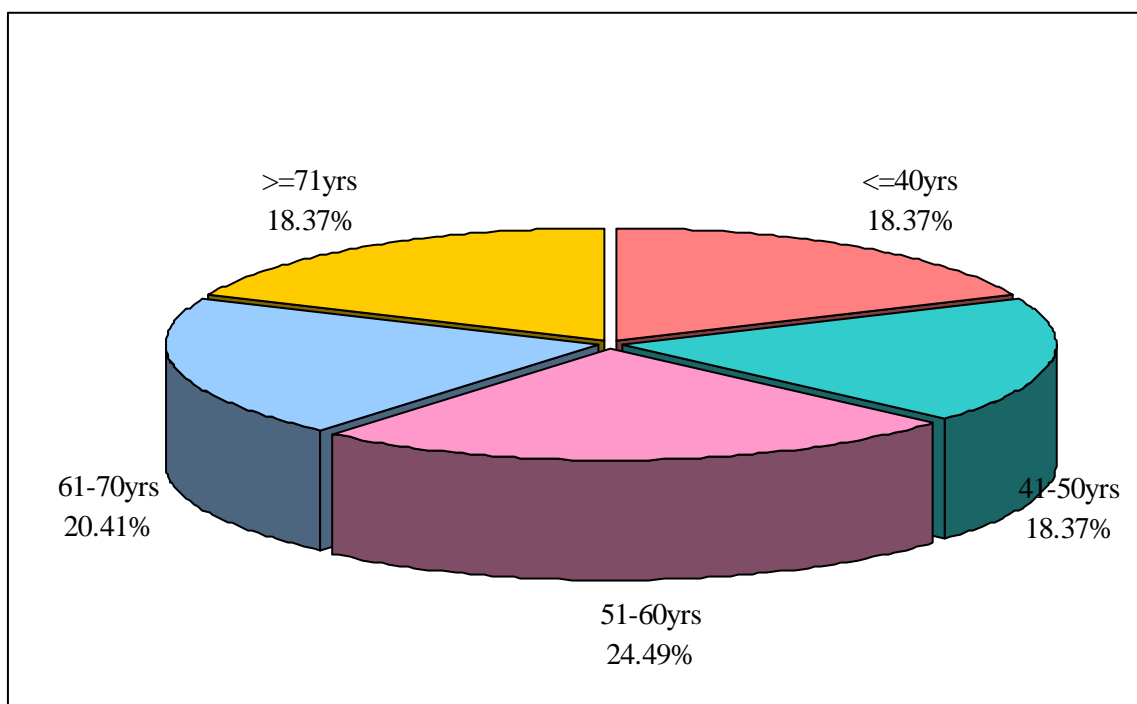


Table 4: Categorization of the benign and malignant lymph nodes by age groups

Age groups	Benign	%	Malignant	%	Total	%
<=40yrs	6	22.22	3	13.6	9	18.36
41-50yrs	5	18.51	4	18.18	9	18.36
51-60yrs	5	18.51	7	31.81	12	54.54
61-70yrs	8	29.62	2	9.09	10	45.45
>=71yrs	3	11.11	6	27.27	9	18.36
Total	27	100	22	100	49	100
Mean age	52.07		58.09			
SD age	18.50		17.14			
Chi-square= 5.593 P = 0.2320						

Graph 2: Bar chart depicting categorization of the benign and malignant lymph nodes by age groups

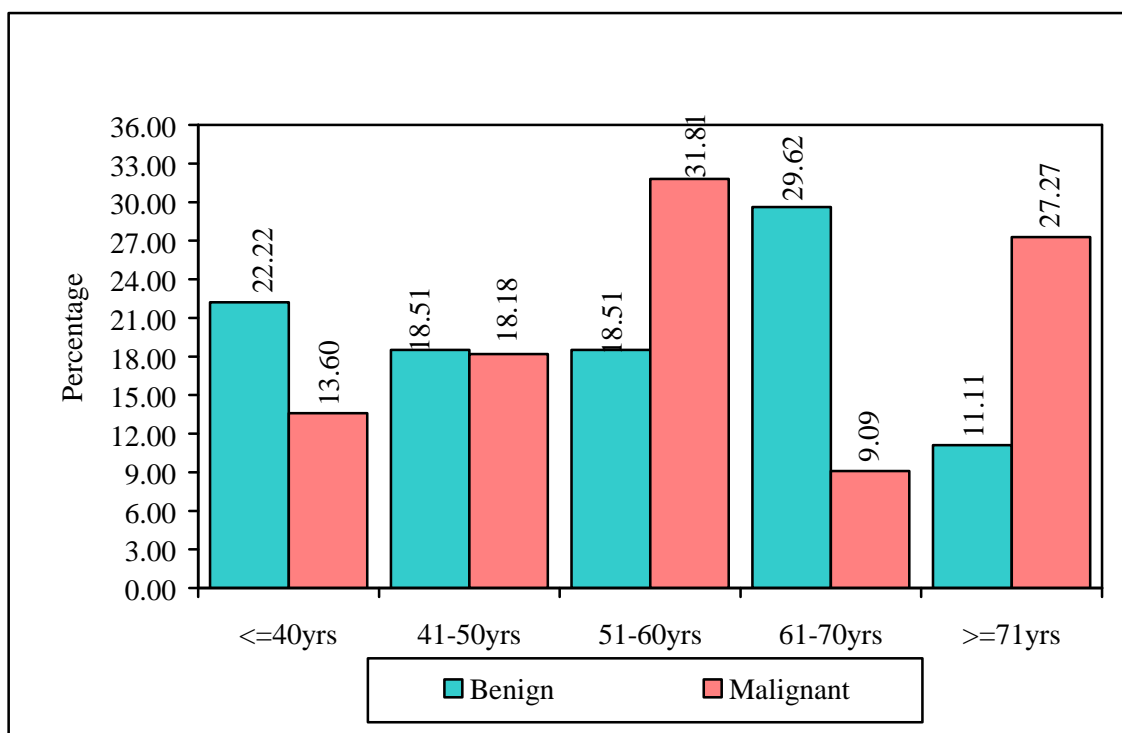


Table 5: Level of the largest nodes studied and its distribution

Largest level of the suspicious node	Number of patients	Percentage
Left Ib	6	12.24
Left II	8	16.32
Left V	2	4.08
Left VIII	1	2.04
Right Ib	11	22.44
Right II	17	34.7
Right III	2	4.0
Right IVb	1	2.02
Right VIII	1	2.02
Total	49	100

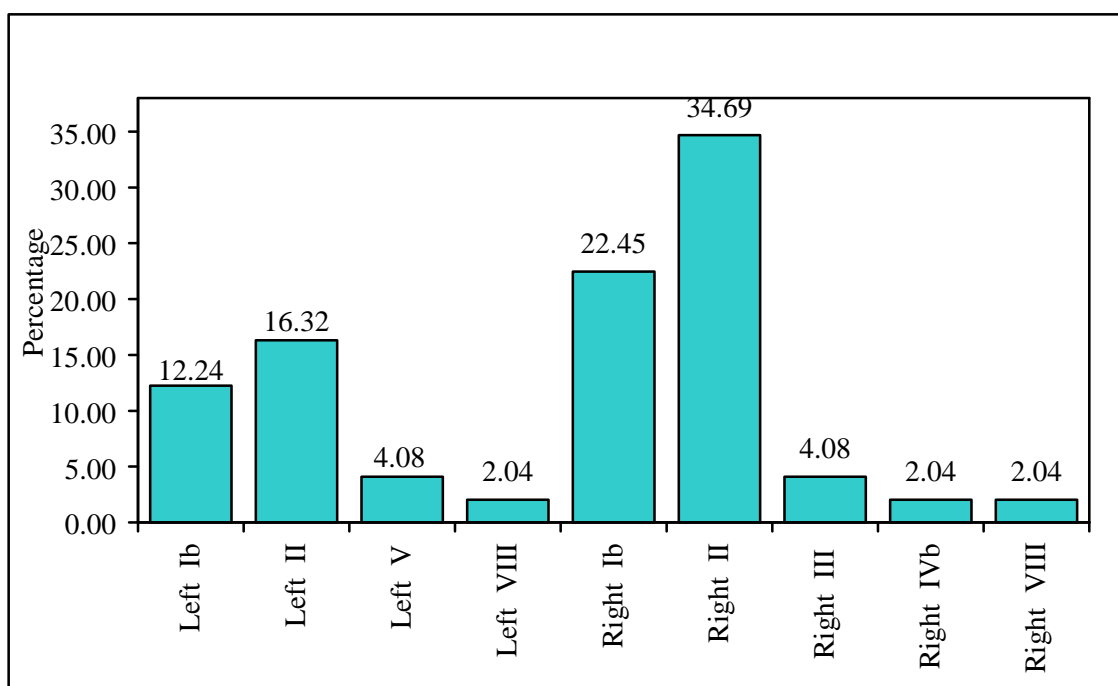
Graph 3: Bar chart showing level wise distribution of the lymph nodes

Table 6: Benign and malignant lymph nodes characterization by largest level

Largest level	Benign	%	Malignant	%	Total	%
Left Ib	4	14.81	2	9.0	6	12.24
Left II	3	11.11	5	22.72	8	16.32
Left V	2	7.40	0	0	2	4.08
Left VIII	0	0	1	4.54	1	2.04
Right Ib	7	26.0	4	18.18	11	22.44
Right II	10	37.03	7	31.81	17	34.7
Right III	0	0	2	9.0	2	4.0
Right IVb	1	3.7	0	0	1	2.02
Right VIII	0	0	1	4.54	1	2.02
Total	27	100	22	100	49	100

Graph 4: Bar chart depicting level wise distribution of the lymph nodes into benign and malignant categories

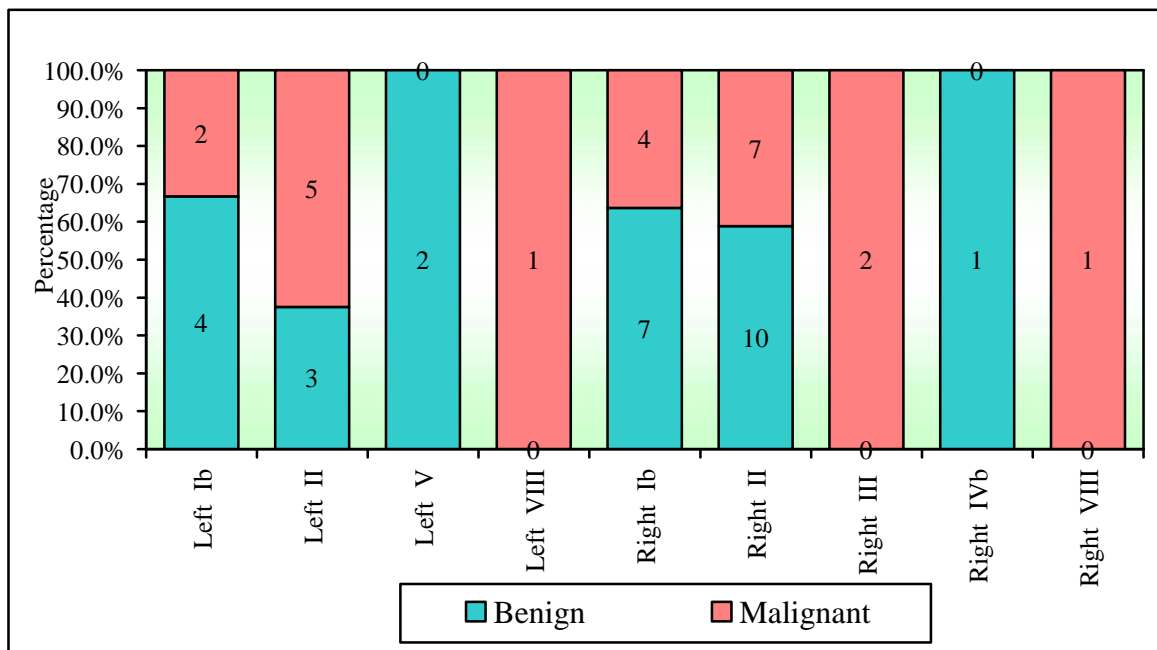


Table 7: Comparison of final diagnosis (Benign and malignant) with mean long axis and short axis by ‘t test’

	Final diagnosis	N	Min	Max	Mean	SD	t-value	p-value
Long axis	Benign	27	1.00	3.20	1.58	0.54	-2.9581	0.0048*
	Malignant	22	1.00	3.50	2.08	0.65		
	Total	49	1.00	3.50	1.80	0.63		
Short axis	Benign	27	0.50	2.80	0.90	0.45	-4.1501	0.0001*
	Malignant	22	0.50	2.70	1.54	0.62		
	Total	49	0.50	2.80	1.19	0.61		

*p<0.05

Graph 5: Bar chart showing comparison of final diagnosis (Benign and malignant) with mean long axis and short axis dimensions

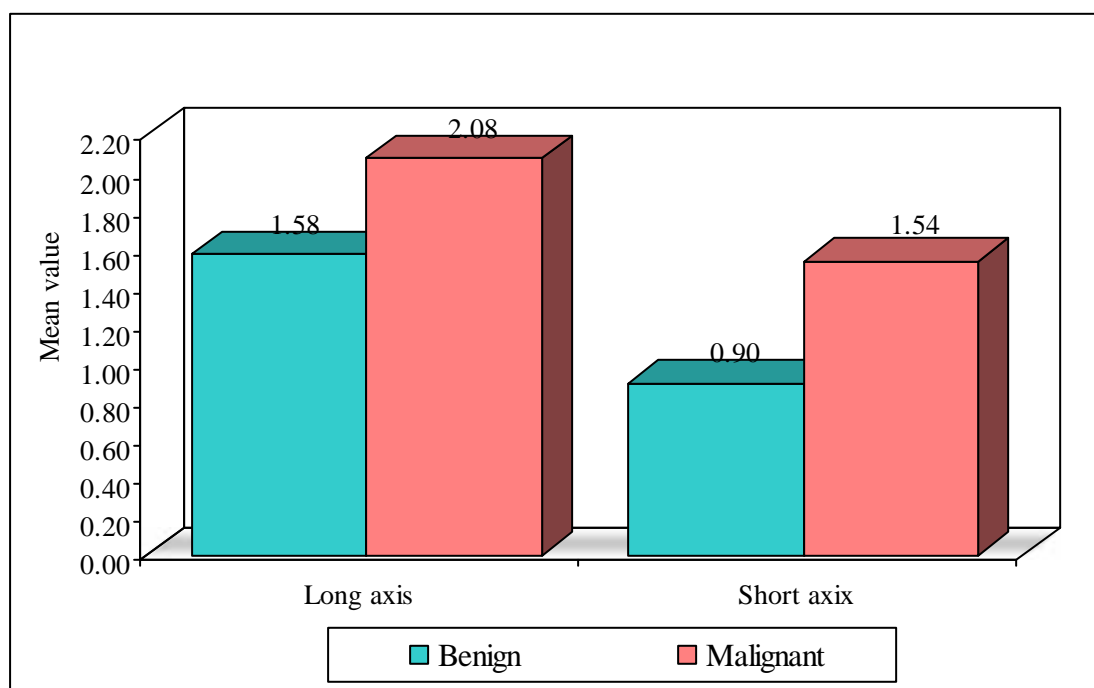


Table 8: Comparison of final diagnosis (Benign and malignant) with mean L/S ratio by ‘t test’

Final diagnosis	N	Min	Max	Mean	SD	t-value	p-value
Benign	27	1.14	2.80	1.86	0.45	3.2218	0.0023*
Malignant	22	1.00	2.33	1.46	0.43		
Total	49	1.00	2.80	1.68	0.48		

*p<0.05

Graph 6: Bar graph showing Benign and malignant lymph nodes categorization with mean L/S ratio

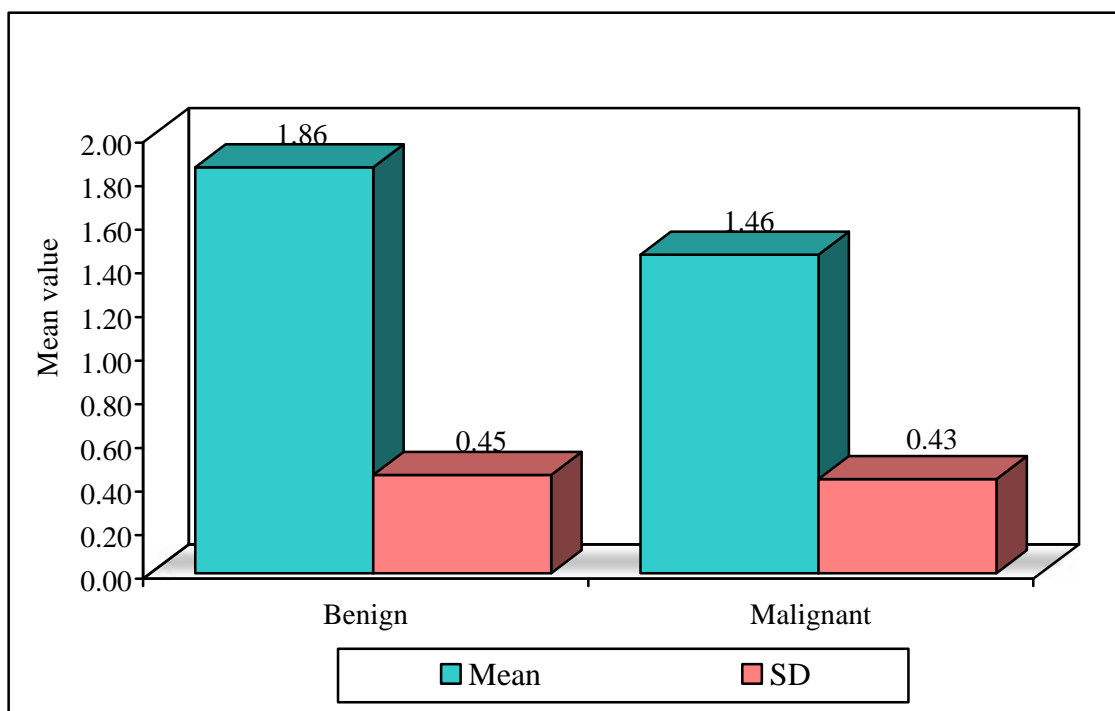


Table 9: Shape wise distribution of the LN

Shape	Number	Percentage
Oval	37	75.51
Round	12	24.49
Total	49	100.00

Graph 7: Pie chart showing the shape wise distribution of nodes

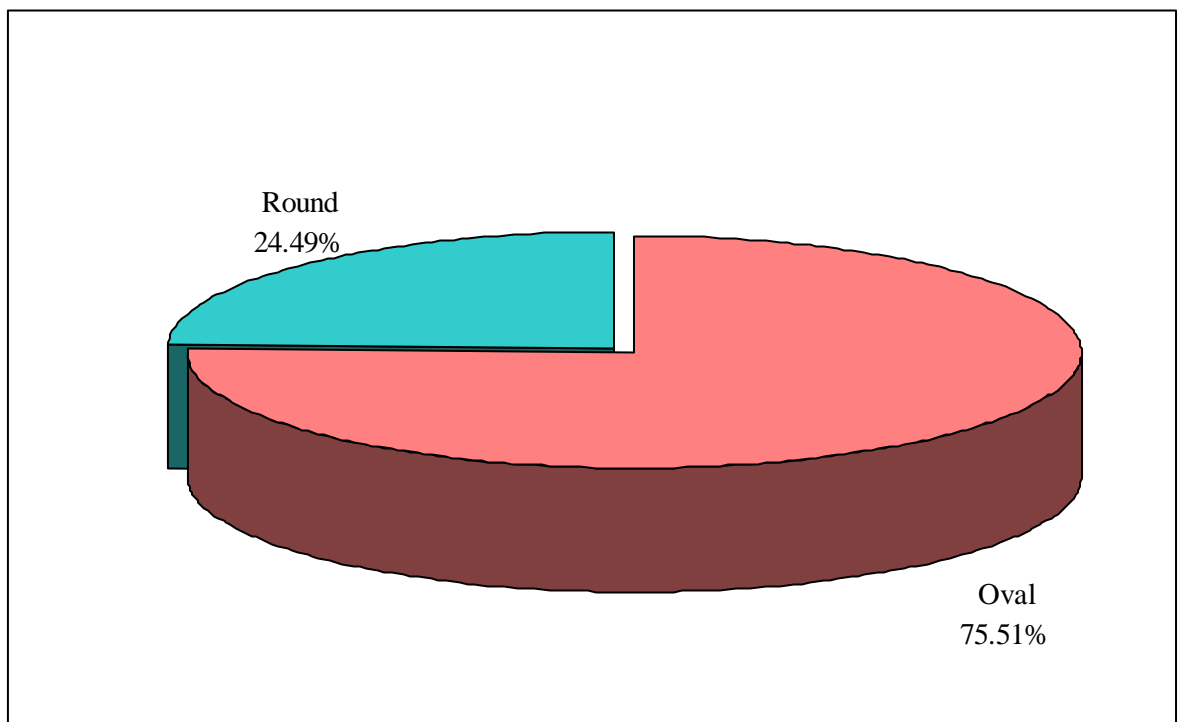


Table 10: Comparison of the final diagnosis with shape of the nodes

Shape	Benign	%	Malignant	%	Total	%
Oval	27	100.00	10	45.45	37	75.51
Round	0	0.00	12	54.55	12	24.49
Total	27	100.00	22	100.00	49	100.00

Chi-square with Yates's correction = 19.5042 P = 0.0001*

*p<0.05

Graph 8: Bar graph depicting the shape wise distribution of nodes

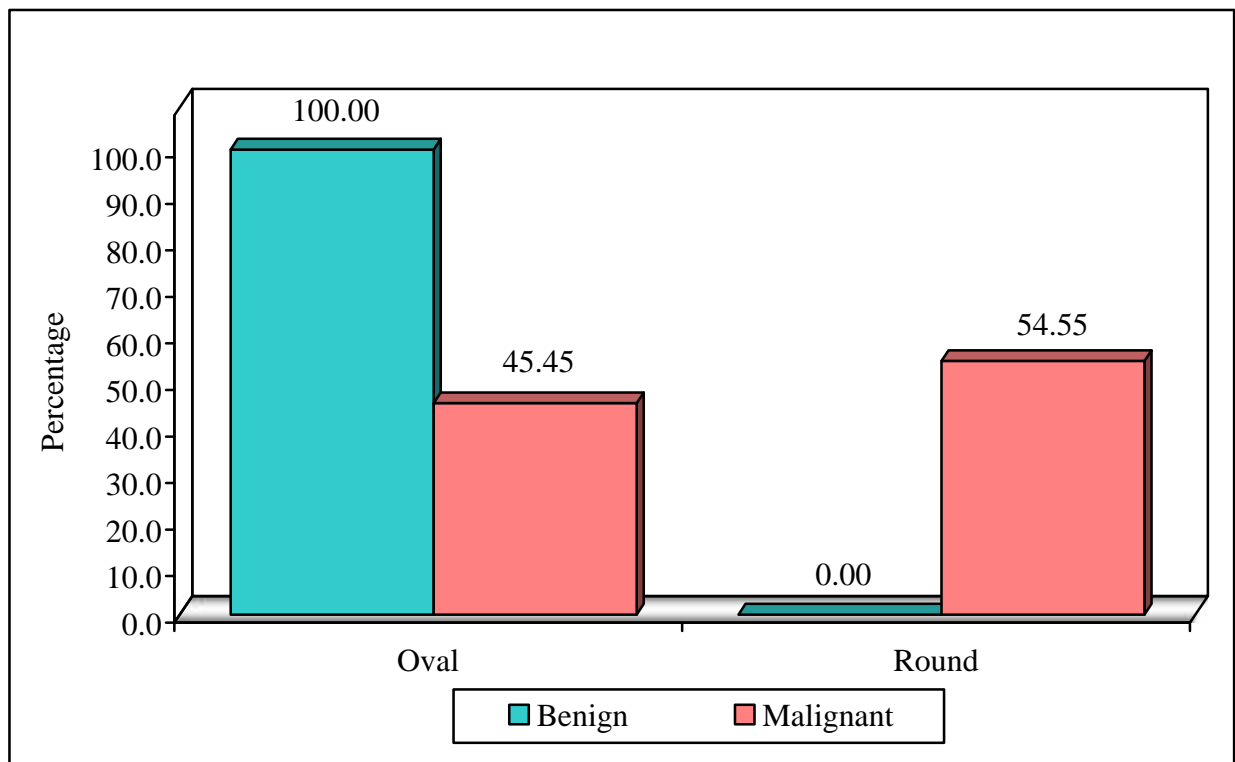


Table 11: Distribution of the nodes depending on the margins

Margins	Number	Percentage
Well defined	40	81.63
Ill defined	9	18.37
Total	49	100.00

Graph 9: Pie chart showing distribution of the nodes depending on the margins

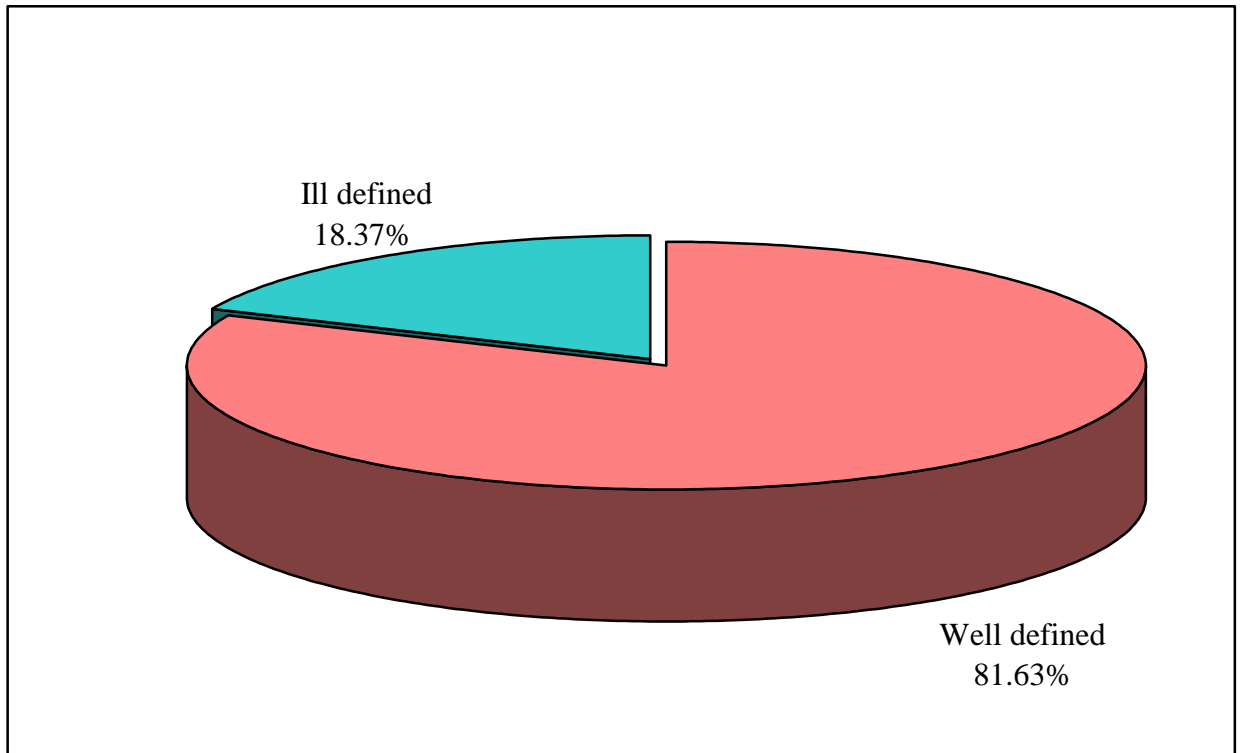


Table 12: Comparison of the final diagnosis with the margins of the nodes

Margins	Benign	%	Malignant	%	Total	%
Well defined	27	100.00	13	59.09	40	81.63
Ill defined	0	0.00	9	40.91	9	18.37
Total	27	100.00	22	100.00	49	100.00

Chi-square with Yates's correction = 10.9401 P = 0.0010*

*p<0.05

Graph 10: Bar graph showing characterization of the nodes depending on the margins

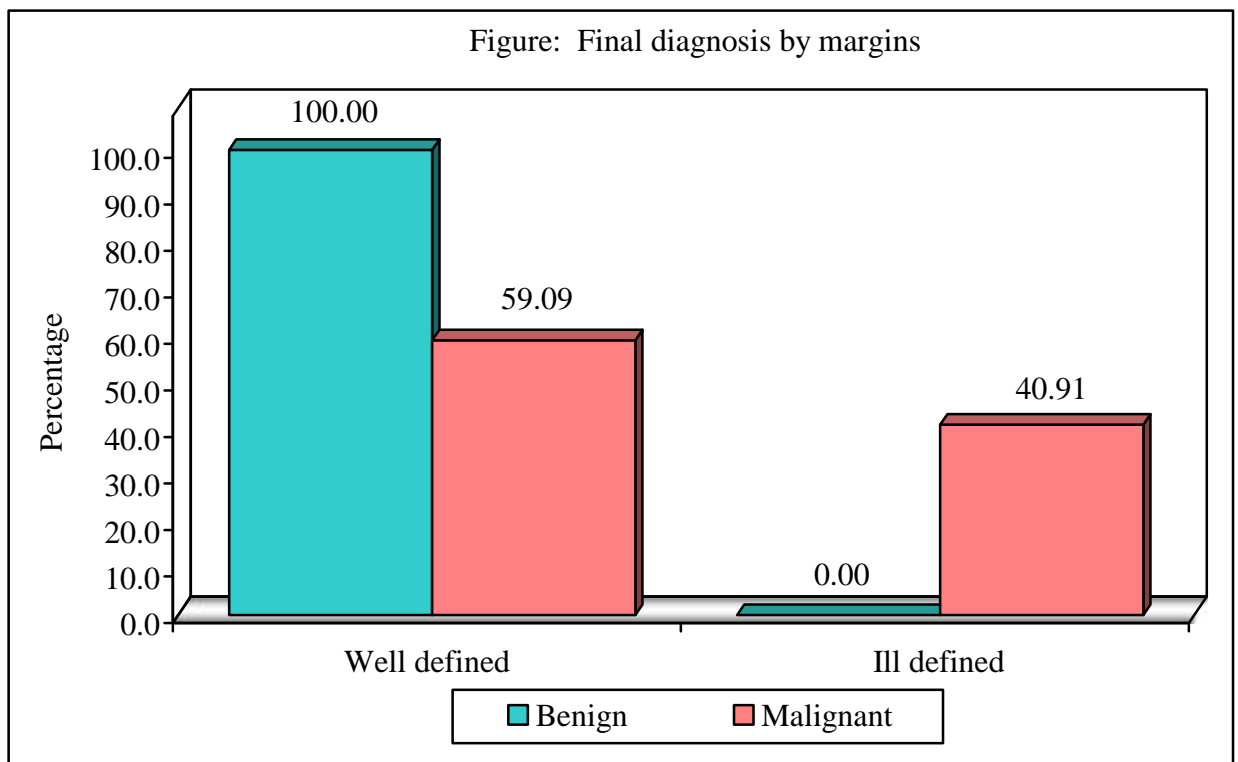


Table 13: Necrosis wise distribution of the LNs

Necrosis	Number	Percentage
Absent	44	89.80
Present	5	10.20
Total	49	100.00

Graph 11: Pie chart showing distribution of the nodes depending on the necrotic changes within the nodes

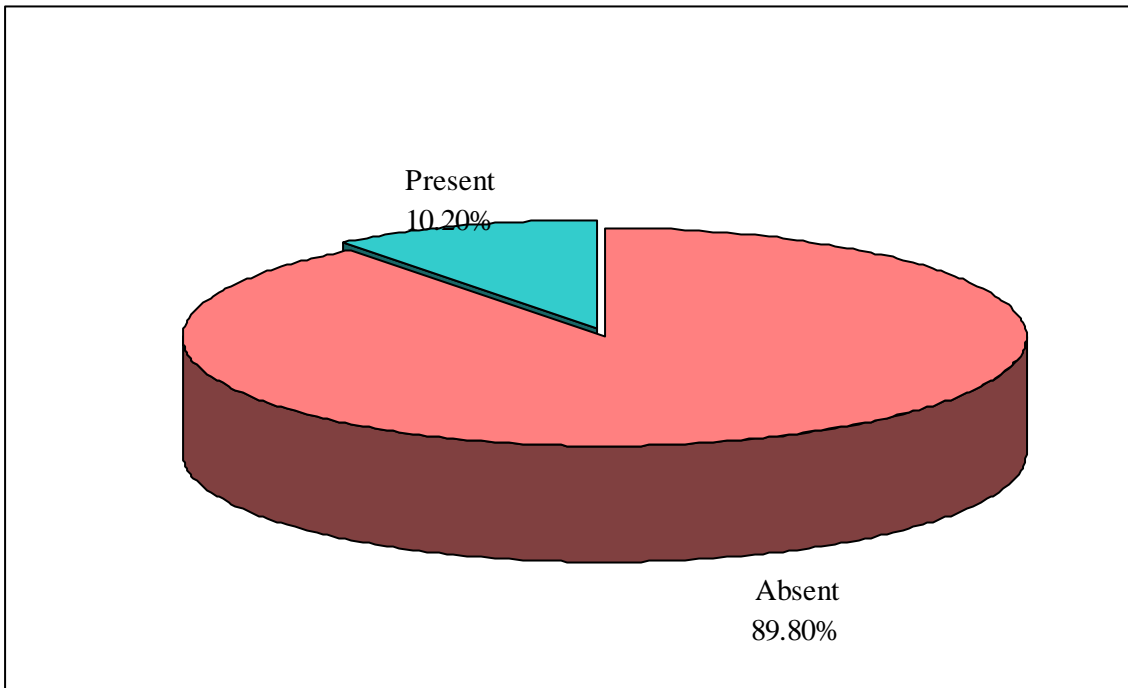


Table 14: Comparison of the final diagnosis with the necrotic changes in the nodes

Necrosis	Benign	%	Malignant	%	Total	%
Absent	26	96.30	18	81.82	44	89.80
Present	1	3.70	4	18.18	5	10.20
Total	27	100.00	22	100.00	49	100.00

Chi-square with Yates's correction = 1.4180 P = 0.2340

Graph 12: Bar graph showing categorization of the nodes on the basis of necrotic changes

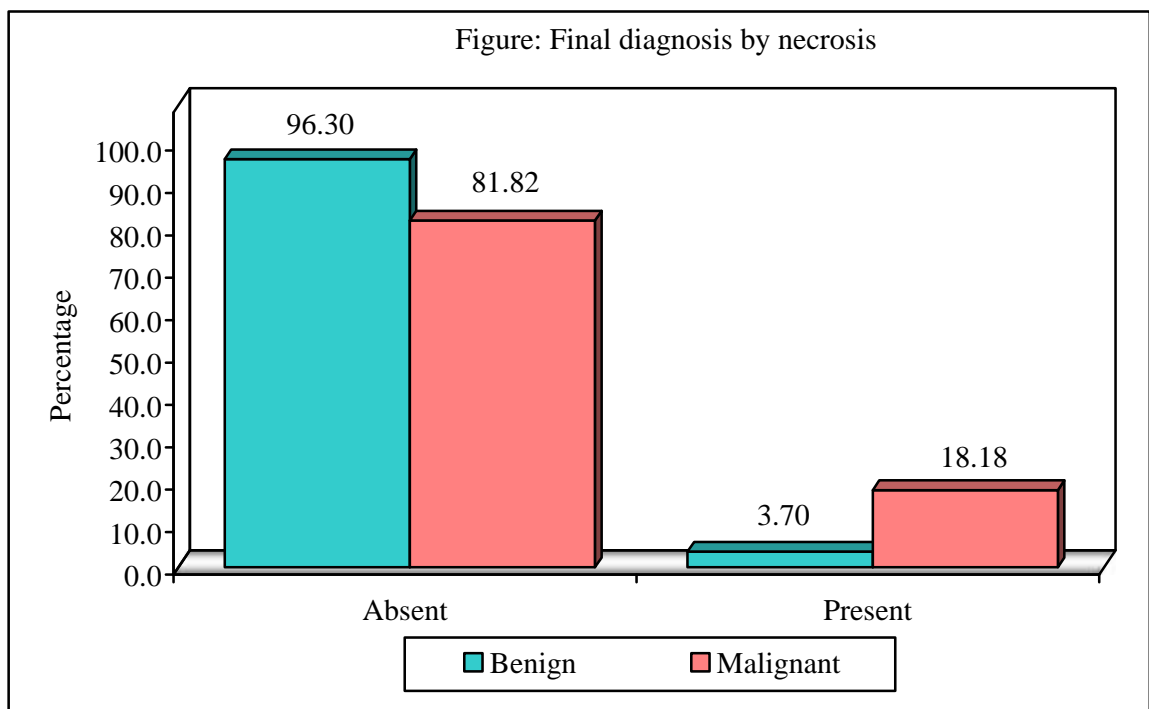


Table 15: Differentiation of the nodes depending on the status of the fatty hilum

Fatty hilum	Number	Percentage
Maintained	31	63.27
Loss of fatty hilum	18	36.73
Total	49	100.00

Graph 13: Pie chart showing distribution of patients depending on the status of the fatty hilum of the nodes

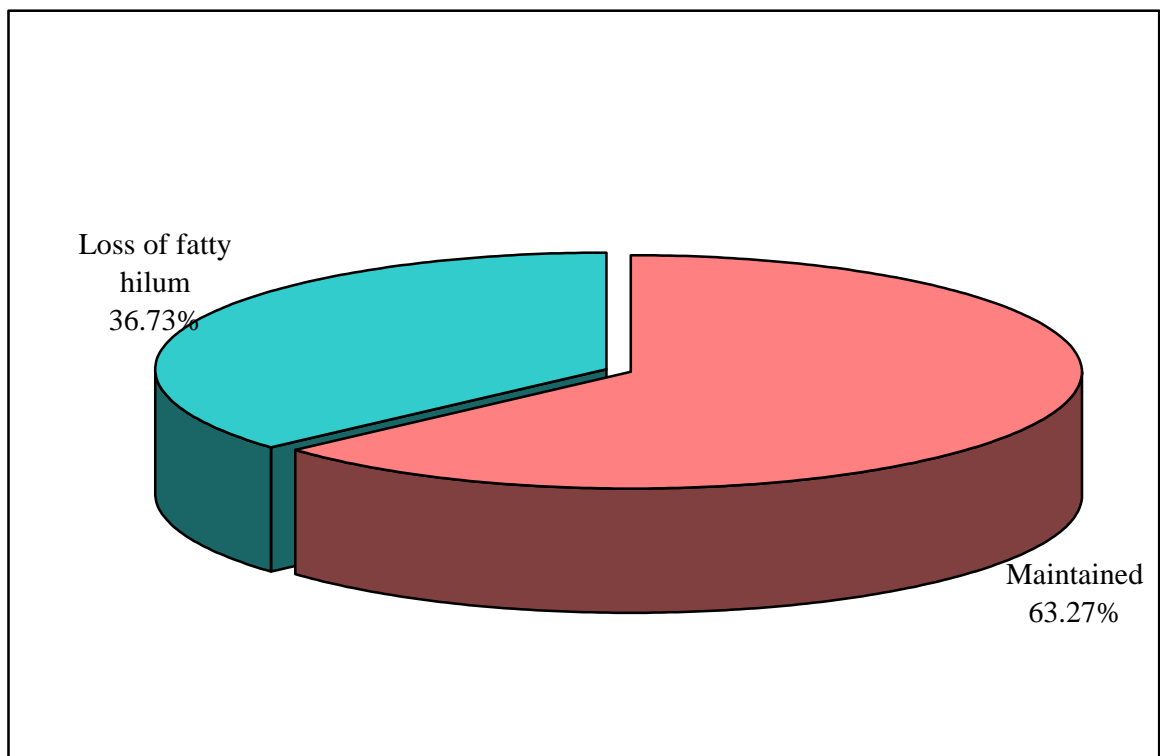


Table 16: Comparison of the final diagnosis with the status of fatty hilum of the nodes

Fatty hilum	Benign	%	Malignant	%	Total	%
Maintained	26	96.30	5	22.73	31	63.27
Loss of fatty hilum	1	3.70	17	77.27	18	36.73
Total	27	100.00	22	100.00	49	100.00
Chi-square=28.2322 P = 0.0001*						

*p<0.05

Graph 14: Bar graph showing categorization of the nodes depending on the preservation or loss of fatty hilum of the nodes

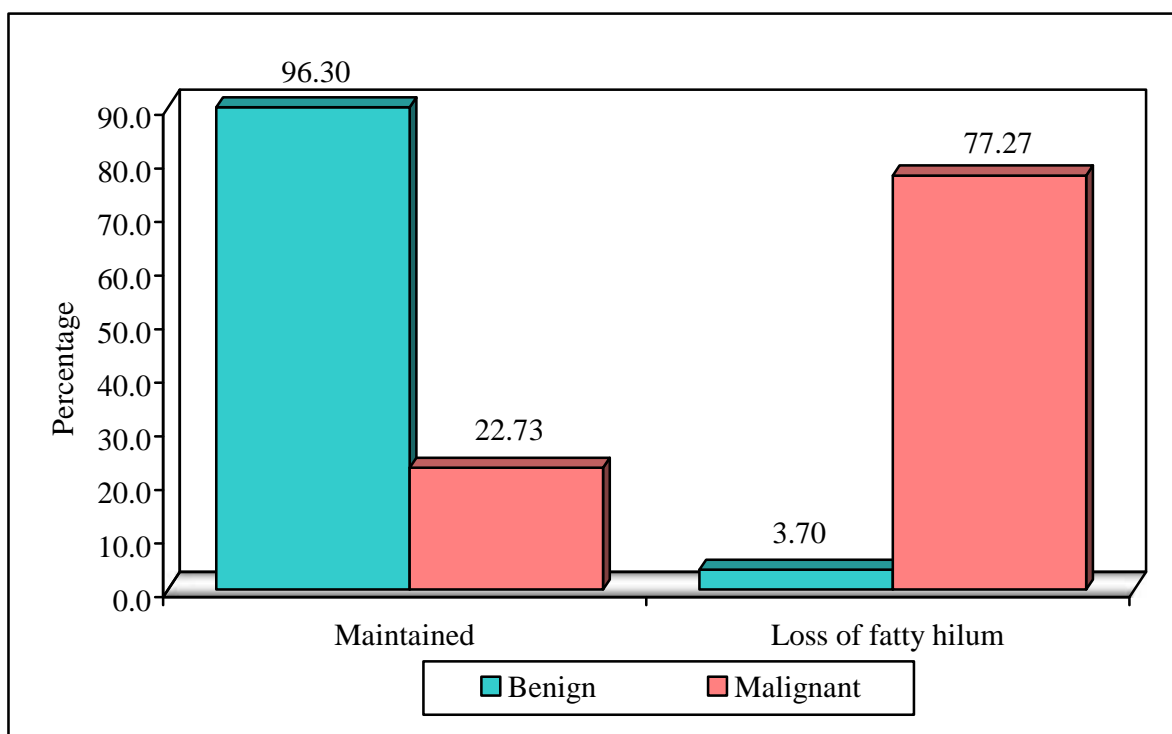


Table 17: Short axis wise distribution

Short axis	Number	Percentage
Subcentimetric	22	44.90
Enlarged	27	55.10
Total	49	100.00

Graph 15: Pie chart showing distribution of patients depending on the largest dimension of the short axis of the nodes

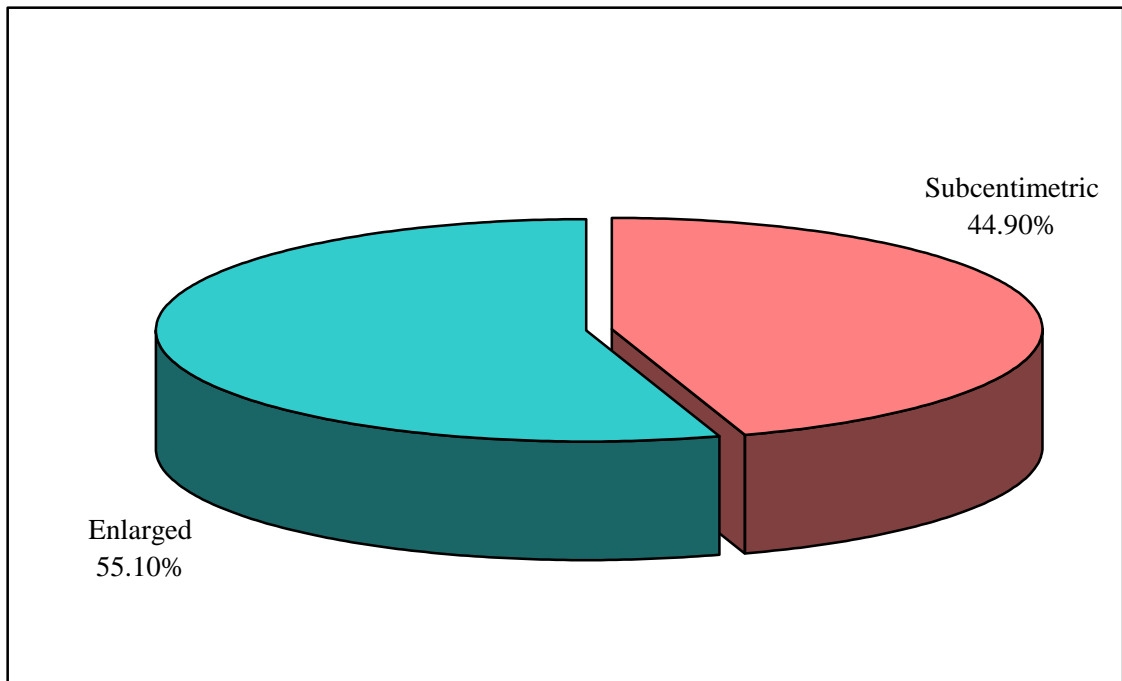


Table 18: Comparison of the final diagnosis with the largest short axis dimension of the nodes

Short axis	Benign	%	Malignant	%	Total	%
Subcentimetric	18	66.67	4	18.18	22	44.90
Enlarged	9	33.33	18	81.82	27	55.10
Total	27	100.00	22	100.00	49	100.00

Chi-square=11.5192 P = 0.0010*

*p<0.05

Graph 16: Pie chart showing categorization of the nodes depending on the largest short axis dimension of the nodes

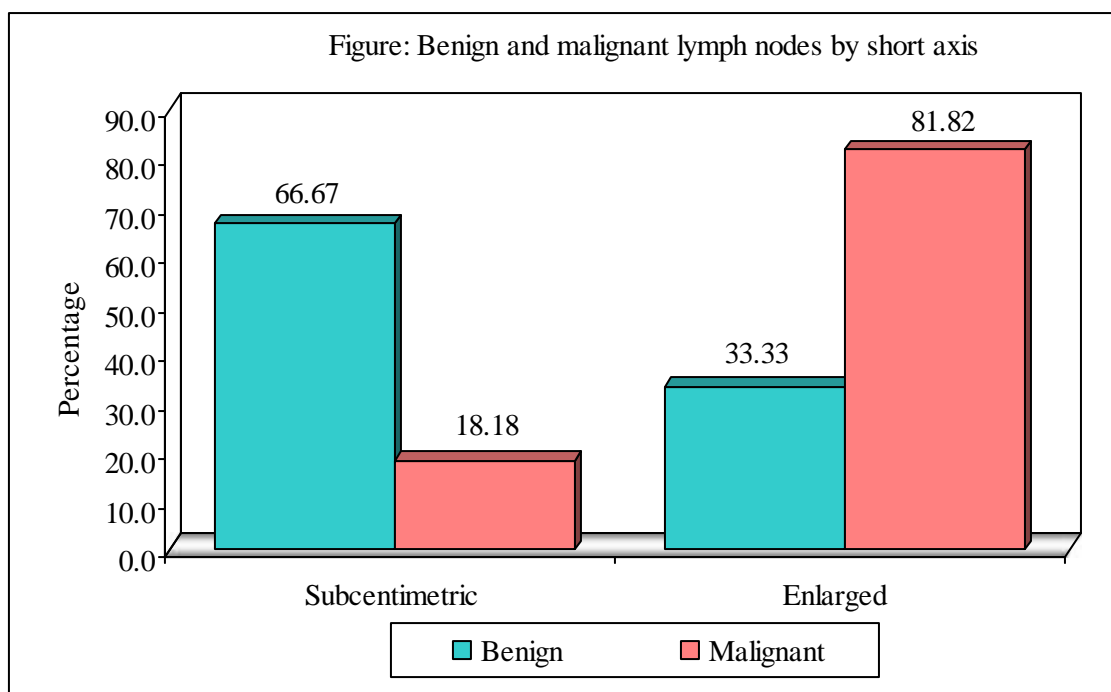


Table 19: Distribution of the nodes depending on the diffusion restriction on DWI

DWI	Number	Percentage
No restriction	25	51.02
Shows restriction	24	48.98
Total	49	100.00

Graph 17: Pie chart showing distribution of nodes depending on the presence or absence of the diffusion restriction seen on DWI in the nodes

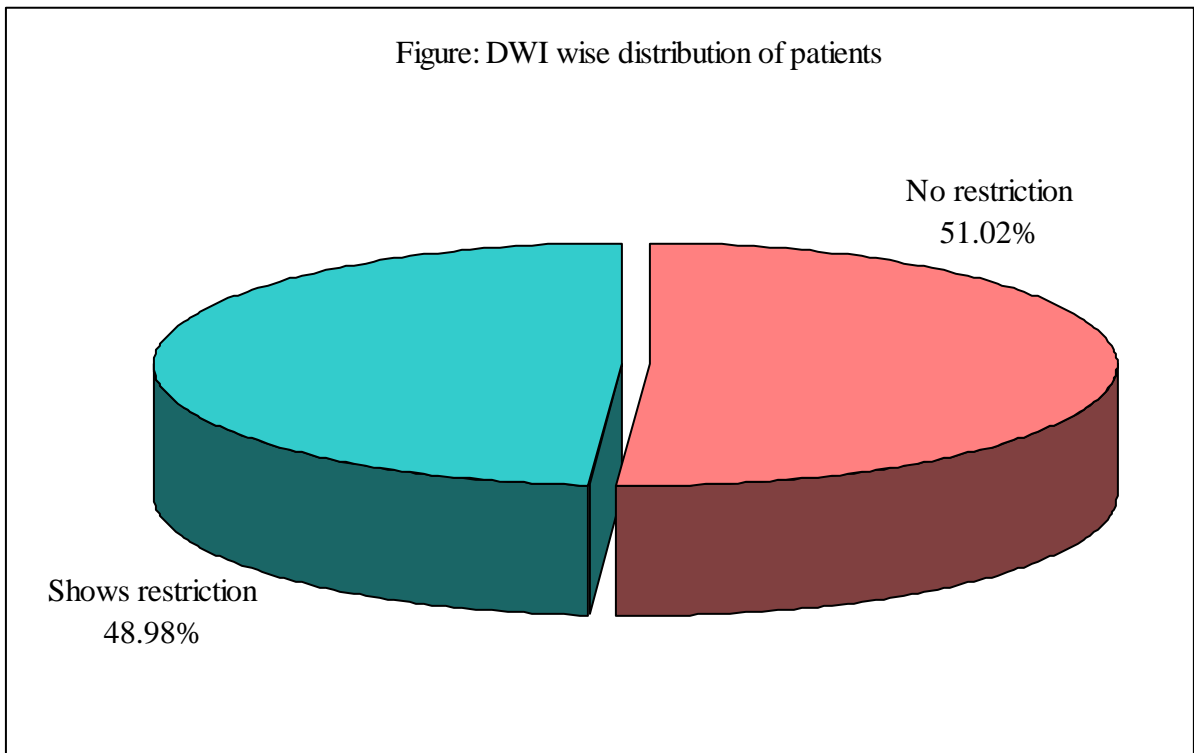


Table 20: Comparison of the final diagnosis with the status of diffusion restriction of the nodes on DWI sequence

DWI	Benign	%	Malignant	%	Total	%
No restriction	21	77.78	4	18.18	25	51.02
Shows restriction	6	22.22	18	81.82	24	48.98
Total	27	100.00	22	100.00	49	100.00
Chi-square=17.229 P = 0.0.0001*						

*p<0.0

Graph 18: Bar graph showing categorization of the nodes depending on the status of diffusion restriction of the nodes on DWI sequence

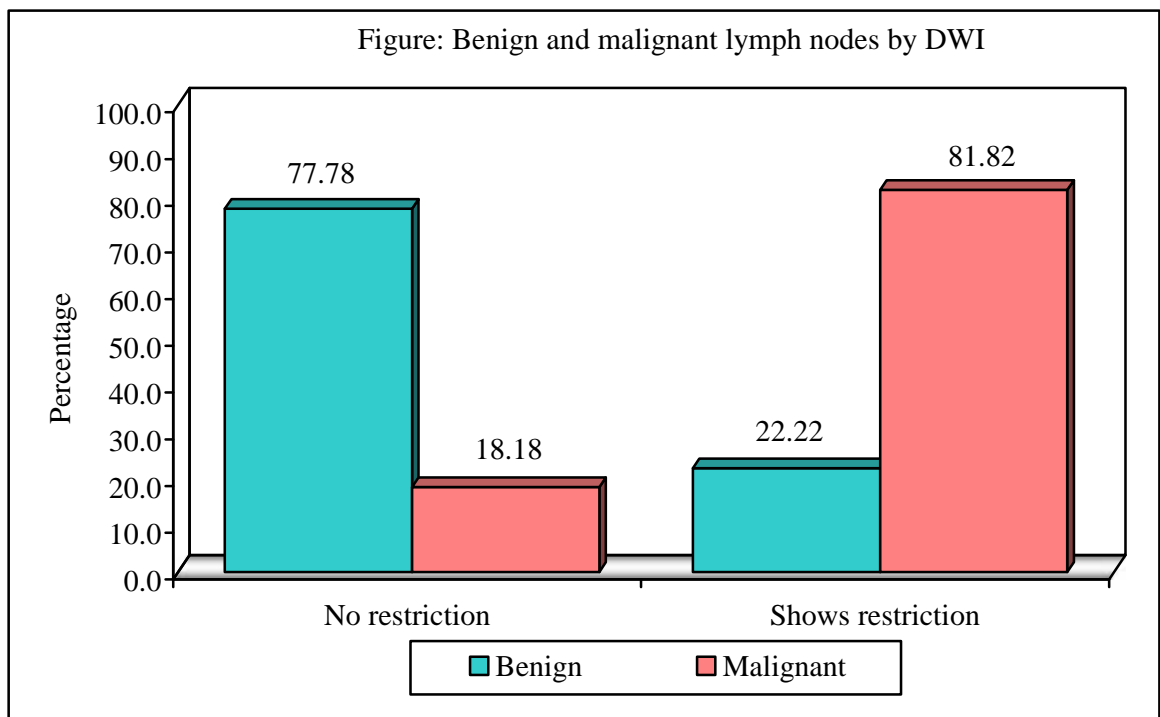


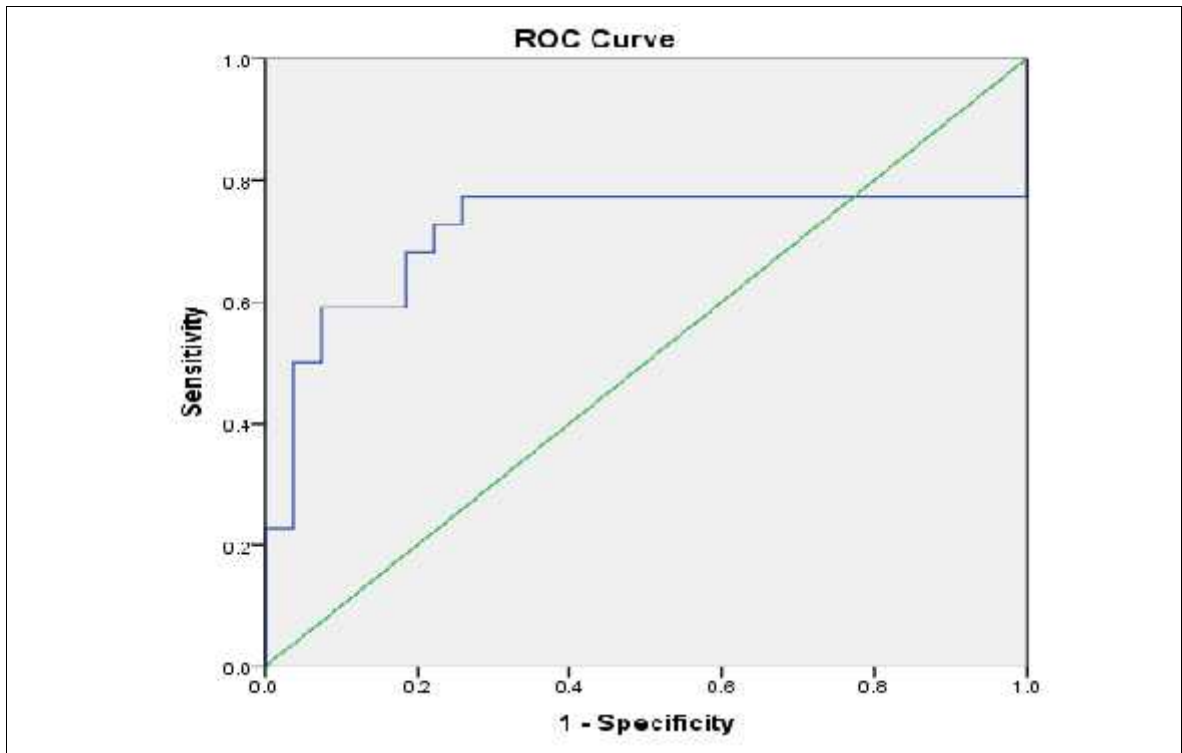
Table 21: Comparison of final diagnosis (Benign and malignant) with mean ADC value by “t test”

Final diagnosis	N	Min	Max	Mean	SD
Benign	27	822.8	1342.2	1145.0	109.1
Malignant	22	550.8	2723.7	1116.5	506.3
Total	49	550.8	2723.7	1132.2	344.6

Table 22: Sensitivity, specificity, PPV, NPV and Accuracy of ADC values in differentiation of the nodes into benign and malignant categories.

Statistic	Value	95% CI
Sensitivity	59.09%	36.35% to 79.29%
Specificity	92.59%	75.71% to 99.09%
Positive Predictive Value	86.67%	62.10% to 96.27%
Negative Predictive Value	73.53%	62.44% to 82.27%
Accuracy	77.55%	63.38% to 88.23%

Graph 19: Receiver operating characteristic (ROC) curve of the ADC values used for differentiating benign from malignant lymph nodes.



The area under the curve of 0.7170, hence we obtained the threshold ADC value for differentiating benign from malignant nodes from this ROC curve = $1.023 \times 10^{-3} \text{ mm}^2/\text{s}$.

DISCUSSION

The aim of our study is to differentiate the cervical LNs into benign and malignant etiology based on the DW-MR imaging and the ADC values and to correlate it with the FNAC/ histopathological diagnosis.

Cervical lymphadenopathy is one of the most common conditions in patients presenting to hospital with history of neck swelling or head and neck lesions. The common causes being infectious, metastatic, benign and reactive lymphadenitis. Hence it is necessary to differentiate the nodes for planning of further management. And MRI is the best non-invasive modality for the characterization. Head and neck cancer represent one of the most common cancers worldwide. Greater than 90 percent of cancers in the neck region are of squamous cell origin (HNSCC) which are commonly seen to originate from the mucosa of oral cavity and are commonly known to metastasize to the regional areas of lymphatic chains. The timely detection of such metastasis makes a great difference to the treating oncology surgeon.

In our study, 49 patients with suspected enlargement of the neck nodes underwent MRI screening before biopsy or FNAC for deciding the treatment plan. Patients lost to follow-up and those with imaging artifacts obscuring the characterization of the nodes were excluded from this study. The categorical variables considered in our study are: age, gender, level, size, shape, margins, preservation of fatty hilum & morphology, necrosis, diffusion restriction on DWI, ADC values and final diagnosis. Final diagnosis was by histopathology / FNAC results. Taking into consideration the histopathological/ FNAC results as the final diagnosis, 22 (44.9 %) patients had malignant nodes and 27 (55.10%) had benign nodes. 23 patients included in this study group had neck carcinomas with metastatic LNs, out of which

16 were from Squamous cell carcinoma of tongue, 3 from carcinoma buccal mucosa, 2 from mucoepidermoid carcinoma of parotid glands, 1 with squamous cell carcinoma (SCC) of cheek, 1 from glottis (laryngeal) carcinoma, 1 patient presented with Non-Hodgkin lymphoma and 17 patients with benign nodes, 1 patient with tuberculous lymphadenitis and 7 with reactive lymphadenitis.

The association of ADC with type of LNs were assessed using a chi-squared test. The mean ADC values between were compared using a student t-test. ROC was plotted of the ADC numerical values and accuracy was calculated.

AGE WISE DISTRIBUTION:

Patients between 10 to 90 years of age were included and the patients were categorized depending on the study diagnosis which was given by the ADC values of the studied node. The mean age of patients presenting with benign nodes was 52.07 years with a SD of 18.50 and that of malignant was 58.09 years with a SD of 17.14 with a distribution of 6 patients in benign category of age less than or equal to 40 years, 5 in the interval of 41-50 years, 5 in the interval of 51-60 years, 8 between 61-70 years & 3 of age more than or equal to 71 years and in malignant category; 3 of age less than or equal to 40 years, 4 patients between 41-50 years, 7 between 51-60 years, 2 between 61-70 years and 6 of age more than or equal to 71 years.

LEVEL WISE DISTRIBUTION OF THE LARGEST LN:

The levels of the largest lymph nodes taken into consideration for its correlation with FNAC/ HPR reports showed maximum involvement of right level II nodes. 100% nodes of level IVb and V on left side were benign. Maximum number of malignant nodes was found in level II group (51.02%) with right side involvement

more than left side. Maximum number of malignant lymph nodes involvement was found in level II secondary to metastases from regional primaries suggesting that H&N carcinomas have a higher predilection to metastasize to level II nodes. Malignant LN were found in larger number at levels I and II. No malignant nodes were noted in level IVb (supraclavicular) and V.

Dr. Choure A. A. et al. assessed 41 nodes in his study, out of which 22 (53.7%) were present at the level II, 10 (24.32%) were seen in the level III, 2 (4.9%) were seen each at level Ib, IV, Va, and Vb and least 1 (2.4%) lymph node was at the level Ia. No benign node was seen at level VI and VII in this group. Out of 30 malignant lymph nodes assessed 17 (56.7%) were present at level II, 8 (26.7%) were noted at level III, 2 were seen each at the level Ib and V and least 1 (3.3%) lymph node was at the level IV. No malignant lymph node was seen at level VI, VII and supraclavicular group in this study.⁴³

Essing H et al also proved that most common metastasis in oral cavity cancers are seen at the level Ib and II.⁴⁴

SIZE:

The size range for maximum short axis dimension of benign lymph nodes ranged from 0.5 cm to maximum of 2.8 cm with a mean of 0.9 cm and standard deviation of 0.45 and that of malignant nodes ranged from 0.5 cm to maximum of 2.7 cm with a mean of 1.54 cm and SD of 0.62 with a p value of 0.0001. The long axis: short axis ratio (L/S ratio) for the benign and malignant nodes ranged from 1.14 to 2.8 for benign and 1.0 to 2.3 for malignant with a mean of 1.86 for benign and 1.46 for malignant respectively (p value=0.0023), proving the study to be significant.

Curtin O. et al. evaluated the sensitivity and specificity of different size criteria for HNSCC metastases and reported size cut-off value of the largest short axial diameter to be “1 cm” for the characterization of the nodes based on size criteria and achieved 88% sensitivity and 39% specificity, whereas a cut-off value of “1.5 cm” for short axis evaluation resulted in 56% sensitivity and 84% specificity.⁴⁵

SHAPE WISE DISTRIBUTION:

Out of the 49 nodes studies, 37 nodes that were studied were oval in shape and 12 were rounded. Of the 27 benign lymph nodes studied, all were oval in shape (100%) which suggested that benign nodes are always oval in shape. Of the 22 malignant nodes, 10 (45.45%) were oval and 12 (54.55%) were rounded which showed characteristic correlation and significant p value of 0.0001.

These findings were correlated with Dr. Choure A A et al study which showed 92.2% of the benign nodes to be oval and 83.3% malignant nodes were rounded.⁴³

MARGINS:

Out of 49 nodes, 40 (81.63%) had well defined margins and 9 (18.37%) had ill defined margins. All the 27 benign nodes are seen to have well circumscribed margins (100%). Out of 22 malignant nodes, 13 (59.09%) had well circumscribed margins and 9 (40.91%) showed ill defined margins. These 9 malignant nodes that showed ill defined margins, when resected showed extracapsular extension on histopathology. The study holds significance with a p value of 0.0010 suggesting that all the benign nodes have maintained well defined margins and the malignant nodes with irregular margins suggest the extracapsular spread of the metastases.

This was compared to the study done by Dr. Choure A A et al which showed 90.2 % benign nodes had smooth margins and 4% crenulated margins and 83.3% malignant nodes had irregular margins and 9.8% had regular margins.⁴³

NECROSIS:

Of 49 nodes studied, 44 (89.90%) nodes did not have necrosis whereas 5 (10.20%) had necrosis. 27 benign nodes, 26(96.30%) had no signs of necrosis whereas 1 (3.70%) had and of the 22 malignant nodes, 18 (81.82%) had no signs of necrosis whereas 4 (18.18%) had. Out of the 5 necrotic nodes, 4 (80%) were malignant and 1 (20%) was benign. The benign node which showed necrosis was secondary to tuberculosis infection.

This result in comparison with the study done by Y. Zhang et al showed dissimilar finding in which he found 31.2% of the malignant nodes to be necrotic and 72% of the tubercular nodes to be necrotic.⁴⁶

It did not correlate well with the study done by Dr. Choure et al. which showed 90.0% of the malignant nodes with necrosis and 4% without necrotic changes whereas, 90.2% of the benign nodes had no signs of necrosis and 3% had necrotic changes.⁴³

FATTY HILUM:

Out of 49 nodes, 31 (63.27 %) nodes showed maintained fatty hilum and 18 (36.73%) showed loss. Of the 27 benign nodes, 26(96.30%) showed maintained fatty hilum whereas 1 (3.70%) showed altered fatty hilum and of the 22 malignant nodes, 5 (22.73%) showed maintained whereas 17 (77.27%) showed altered hilum and showed

a significance of the study with a p value equivalent to 0.0001. The benign node which showed altered fatty hilum was the necrotic node of tubercular origin.

This was compared to the Dr. Choure A A et al study which showed preserved hilum in 87.8 % benign nodes & alteration in 12.2% and preserved hilum in 6.7% of the malignant nodes and alteration in 93.3%.⁴³

SHORT AXIS:

To characterize the nodes as benign or malignant depending on the short axial diameter, cut-off was considered as 1.0 cm. Based on this criteria, out of 49 nodes, 22(44.90 %) nodes turned out to be subcentimetric (with the largest short axis diameter being \leq to 1.0 cm) and 27 (55.10%) turned out to be enlarged (maximum short axis diameter being more than 1.0 cm). Out of 22 subcentimetric nodes, 18 (66.67%) were benign and 4 (18.18%) were malignant (33.33%) and out of 27 enlarged nodes, 4 (18.18 %) were benign and 23 (81.82%) were malignant. This study showed a significant correlation with a p value of 0.0010 to differentiate the nodes depending on the short axial diameter suggesting that 81.82% malignant nodes were enlarged.

In a study conducted by Eisenhauer E.A et.al, nodes having short axis diameter as more than or equal to 15 mm were considered as target lesions. The short axis dimension should be considered to calculate the tumour response. Nodes which shrunk to less than or equal to 10 mm post treatment were taken as non malignant.⁴⁶

RESTRICTION ON DWI AND ADC CORRELATION:

Restriction on diffusion weighted MRI sequence depends of the cellularity of the tissue. The tissues that are highly cellular show hyperintense signals on DWI with corresponding hypointensity on ADC maps. Thus diffusion-weighted imaging helps in categorizing the nodes with high cellularity being malignant. Out of 49 (49.98%) nodes, 24 (48.98%) showed diffusion restriction and 25 (51.02%) showed no restriction. Out of the nodes which showed diffusion restriction, 22 (81.82%) were malignant and 6 (22.22%) were benign and out of 25 which did not show restriction, 21 (77.78%) were benign and 4 (18.18%) were malignant. This study proved to be significant with a p value of 0.0001. The malignant nodes which did not show diffusion restriction had necrotic component and had turned out to be false negative as the ADC maps showed hyperintense signals and high values in the necrotic component.

This study was compared with the study conducted by Dr. Choure A. A. et al, in which 100% malignant nodes showed restriction. No restriction was seen in the 97.6% of the benign nodes.⁴³

On the ADC maps, the ADC values ranged from 0.822×10^{-3} mm²/sec (minimum) and 1.342×10^{-3} mm²/sec (maximum); having a mean of 1.145×10^{-3} mm²/sec and a standard deviation of 109.1 in benign and that in the malignant nodes, ranged from 0.5508×10^{-3} mm²/sec to 2.723×10^{-3} mm²/sec with a mean of 1.116×10^{-3} mm²/sec and a standard deviation of 506.3. The threshold ADC value was 1.023×10^{-3} mm²/sec. Out of the 22 malignant nodes, 4 nodes had central necrosis and hence showed high values, ranging from 1.420×10^{-3} mm²/sec to 2.723×10^{-3} mm²/sec with a mean of 1.766×10^{-3} mm²/sec suggesting the false negatives in the results obtained through ADC. The mean for the malignant nodes

excluding the necrotic nodes was $0.972 \times 10^{-3} \text{ mm}^2/\text{sec}$. 1 among the benign nodes which was found to be of tubercular etiology with necrosis on FNAC correlation had ADC of $1.324 \times 10^{-3} \text{ mm}^2/\text{sec}$. Of the 27 benign nodes, 1 was of tubercular origin and 6 were reactive lymphadenitis. ADC values of the reactive lymphadenitis nodes ranged from $0.822 \times 10^{-3} \text{ mm}^2/\text{sec}$ (minimum) to $1.254 \times 10^{-3} \text{ mm}^2/\text{sec}$ (maximum) with a mean of $1.094 \times 10^{-3} \text{ mm}^2/\text{sec}$. Of the 22 malignant nodes, one showed value of $0.550 \times 10^{-3} \text{ mm}^2/\text{sec}$ which was Non – Hodgkin lymphoma on HPR report. The other 21 nodes were metastatic secondaries. The mean ADC for metastatic nodes was higher than that of the lymphomatous nodes due the high cellularity and high nucleolus to cytoplasmic ratio in the lymphomatous tissues. The lower ADC value in benign etiology is explained by the higher concentration of proteinaceous content secondary to the inflammatory reaction.

The sensitivity, specificity, positive & negative predictive value and accuracy of 59.09%, 92.59%, 86.67%, 75.53%, and 77.55% respectively. ROC curve was plotted to calculate the ADC threshold with an area of 0.7170 under consideration and was found to be $1.023 \times 10^{-3} \text{ mm}^2/\text{sec}$.

AbishG. Y et al in his study got the best threshold value as $1.09 \times 10^{-3} \text{ mm}^2/\text{sec}$ with sensitivity; specificity; PPV and NPV 97%, 89%, 96.9% and 89% respectively. ROC curve was plotted to determine the ADC threshold values with an area of 0.96 ($p < 0.0001$) under consideration for differentiation of LNs.⁴¹

The study was also compared with Dr. Choure A. A. et al. study which had ADC values of the nodes studies ranging from 0.4 to $1.3 \times 10^{-3} \text{ mm}^2/\text{sec}$. The values of malignant nodes were in the range of 0.4 to $0.8 \times 10^{-3} \text{ mm}^2/\text{sec}$ and benign were 0.8 to $1.3 \times 10^{-3} \text{ mm}^2/\text{sec}$ with a mean for benign nodes of $1.1 \times 10^{-3} \text{ mm}^2/\text{sec}$ (0.9 SD) and

that for malignant of $0.7 \times 10^{-3} \text{ mm}^2/\text{sec} (\pm 0.2 \text{ SD})$. The ADC cut off was $0.93 \times 10^{-3} \text{ mm}^2/\text{sec}$ with “sensitivity and specificity” of 97.6% of 100% respectively.⁴³

A study on DWI neck imaging conducted at G.M.C. Patiala showed, out of 60 patients, 41 (68.33 %) cases came out as malignant and 19 (31.67 %) cases came out as benign. The results obtained were 36 true positives, 4 false positives, 15 true negatives and 5 false negatives. The overall sensitivity of DWI for differentiating malignant from benign cervical lymphadenopathy was 87.80% with specificity of 78.95%. The PPV & NPV were 90.00% & 75.00% respectively. The best ADC threshold for distinguishing nodes was $1.005 \times 10^{-3} \text{ mm}^2/\text{sec}$.¹

Y. Zhang et al in his study concluded that the mean ADC of the solid portion of tuberculous nodes was $1.01 \times 10^{-3} \text{ mm}^2/\text{sec}$ and was significantly higher ($p < 0.01$) than metastatic nodes ($0.93 \times 10^{-3} \text{ mm}^2/\text{sec}$) and lymphomatous nodes ($0.64 \times 10^{-3} \text{ mm}^2/\text{sec}$) and thus suggest that the mean ADC values are significant to characterize the nodes into benign, metastatic and lymphomatous infiltration. He also proved that the ADC values in malignant necrotic nodes was $2.02 \pm 0.36 \times 10^{-3} \text{ mm}^2/\text{sec}$ and that of the tubercular etiology was $1.25 \pm 1.02 \times 10^{-3} \text{ mm}^2/\text{sec}$ and was quite significant.⁴⁷

CONCLUSION

- The present study demonstrated that the cervical LNs can be characterized into benign and malignant depending on the morphological characteristics like size, shape, largest short axial diameter on axial sections, margins, necrotic changes, fatty hilum, DWI restriction and ADC values.
- The morphologic features on MRI like oval shape, well circumscribed margins, subcentimetric node, maintained fatty hilum, less than 1.0 cm of largest short axial diameter, absence of necrosis, absent diffusion restriction on DWI and higher ADC values (more than $1.023 \times 10^{-3} \text{ mm}^2/\text{sec}$) are suggestive of benignity. Whereas round shape, ill-defined margins, enlarged node, altered hilum, $> 1 \text{ cm}$ of largest short axial diameter, presence of necrosis, diffusion restriction on DWI and ADC values less than $1.023 \times 10^{-3} \text{ mm}^2/\text{sec}$ are features of malignancy. Sensitivity of ADC value in differentiating the nodes was 59.90%, specificity was 92.59%, PPV and NPV were 86.67% & 75.53% respectively. Overall accuracy of this diagnostic modality was 77.55%.

LIMITATIONS:

1. The major limitation was the limited sample size, due to which the detailed evaluation and further characterization of some of the cases was not possible.
2. The role of confounding features like the age of the individual, gender distribution could not be evaluated again due to limited sample size.
3. Contrast imaging was not a criteria taken into consideration which would increase the diagnostic precision and help in excluding the necrotic nodes with high specificity.

RECOMMENDATIONS:

1. DWI is a non-invasive modality with a higher positive & negative predictive value for characterization of the nodes. These LNs can be further characterized into tubercular etiology, reactive lymphadenitis or nodes with no metastasis in cases of carcinomas depending on the ADC and the other morphological characters. It can also differentiate the metastatic etiology from the lymphomatous nodes.
2. It is non-invasive method with no risk of exposure of the patient to contrast agents or radiation to stage the carcinomas and detect the metastasis.
3. There is a need to conduct more studies with a larger sample size to evaluate the diagnostic utility of the imaging modality in different subgroups of the population.
4. The findings of the study must be generalized with caution, considering the differences in the demographic features of the population, the quality of the equipment used and the experience & skill of the radiologists.

SUMMARY

A prospective observational study was conducted in the Department of Radio-diagnosis of a tertiary care teaching hospital to assess the diagnostic ability of the DW MR imaging in comparison with pathological reports. ADC values proven to be effective in characterizing the nodes into benign and malignant etiology with a sensitivity of 59.90%, specificity of 92.59%, Positive predictive value of 86.6%, negative predictive value of 73.53% and an accuracy of 77.55% suggesting that DWI with ADC maps can be successfully used as an imaging modality for further management of patients.

BIBLIOGRAPHY

1. Mathur M, Duhan V, Gupta R.K, Gupta S, Kaur N, Mathur A. The diagnostic accuracy of diffusion weighted magnetic resonance (MR) imaging for discrimination of malignant from benign cervical lymphadenopathy in head and neck tumours using histopathology as the reference standard. *Int J Med Res Rev* 2017;5 (12):1004-14
2. Kulkarni M R. Head and neck cancer burden in India. *International journal of head and neck surgery*. 2013;4(1):29-35
3. Langendijk J. A, Slotman B. J, vander Waal I, Doornaert P, Berkof J, LeemansC. R. Risk-group definition by recursive partitioning analysis of patients with squamous cell head and neck carcinoma treated with surgery and postoperative radiotherapy. *Cancer*. 2005;104(7):1408–17
4. Perrone A,Guerrisi P, Izzo L, D’Angeli I, Sassi, Mele L.L et. al. – Diffusion-weighted MRI in cervical lymph nodes: Differentiation between benign and malignant lesions. *European Journal of Radiology*. 2009; 77 : 281–86
5. Rouviere H. *Lymphatic Systems of the Head and neck*. AnnArbor. M. I: EdwardsBrothers, 1938;5-28
6. Arlebout Y. F, *Alle de ontloed-*, Genees H.F, Ruysch V, Amsterdam F: Janssoons van Waesberge; 1744.
7. Virchow R. D, *Geschwulste* B.K. Berlin, Germany: August Hirschwald; 1863

8. Morton D. L, Wen D. R, Wong J. H. Technical details of intraoperative lymphatic mapping for early stage melanoma. *Arch Surgery Journal*. 1992;127:392-99.
9. Bree E. D, Tsiaoussis J, Schoretsanitis G. *Hellenic Journal of Surgery* 2018; 90(6): 308-14.
10. Domenico R, Crivellato E. The embryonic origins of lymphatic vessels: an historical review. *British Journal of Hematology*. 2010; 149 (5):669-74.
11. Ruddle NH. Lymphatic vessels and tertiary lymphoid organs. *J Clin Invest* 2014; 124: 953–59.
12. Breslin J. W,¹ Yang Y,¹ Scallan J. P,¹ Sweat R. S, Adderley S. P,¹ and Murfee W. L. Lymphatic Vessel Network Structure and Physiology. *Compr Physiol*. 2018; 9(1): 207–99.
13. Ambrose CT. Immunology's first priority dispute--an account of the 17th-century Rudbeck-Bartholin feud. *Cell Immunology*. 2006; 242: 1-8.
14. Loukas M, Bellary SS, Kuklinski M, Ferraiola J, Yadav A, Shoja M. M et al. The lymphatic system: a historical perspective. *Clinical Anatomy*. 2011; 24: 807–16.
15. Hewson W. Part 2: a description of the lymphatic system in human subjects, and in other animals In: *Experimental Enquiries*. 2012; 1774: 112–04.
16. Aukland K Arnold Heller and the lymph pump. *ActaPhysiol Scand*. 2005; 185: 171–80.
17. Som. P.M. Lymph Nodes of Neck. *Radiology* 1987; 165:593-600

18. Vincent G, Kian A, Wilfried B, Grau C, Marc H, Johannes A. et al. Delineation of the neck node levels for head and neck tumors: A 2013 update. DAHANCA,EORTC, HKNPCSG, NCIC CTG, NCRI, RTOG,TROG consensus guidelines. Radiotherapy and Oncology. 2013.
19. Kaji A. V, T Mohuchy, Swartz J. D. Seminar Ultrasound CT MR 1997; 18(3):220-49.
20. Mack MG, Rieger J, Baghi M, Bisdas S, Vogl TJ. Cervical lymph nodes. European journal of radiology. 2008; 66(3):493-500.
21. Vaid S, Lee YY, Rawat S, Luthra A, Shah D, Ahuja AT. Tuberculosis in the head and neck-a forgotten differential diagnosis. Clinical radiology. 2010; 65(1):73-81.
22. King AD, Ahuja AT, Metreweli C. MRI of tuberculous cervical lymphadenopathy. Journal of computer assisted tomography. 1999; 23(2):244-47.
23. Sakai O, Curtin HD, Romo LV, Som PM. Lymph node pathology: benign proliferative, lymphoma, and metastatic disease. Radiologic Clinics of North America. 2000; 38(5):979-98.
24. N. Fischbein, S. Noworolski, R. Herny, M. Kaplan, W. Dillon, S. Nelson. Assessment of metastatic cervical adenopathy using dynamic contrast-enhanced MR imaging. AJNR Am J Neuroradiology. 2003; 24: 301-11.
25. Tamer F, Taha A. "Neck lymph nodes: Characterization with diffusion-weighted MRI", The Egyptian Journal of Radiology and Nuclear Medicine.2012; 43(2):173-81.

26. M. Ishikawa, Y. Anzai. MR imaging of lymph nodes in the head and neck. *Neuroimaging Clin N Am*, 2004; 14:679-94.
27. King A.D, Tse G.M, Ahuja A.T, Yuen E.H, Vlantis A.C, Nelson E.W. To, et al. Necrosis in metastatic neck nodes: diagnostic accuracy of CT, MR imaging, and US Radiology. 2004; 230: 20-26.
28. V.F. Chang, Y.F. Fan, J.B. Khoo. MRI features of central necrosis in metastatic disease. *Clinical Radiology*. 1996;51:103-09.
29. T. Ferreira. Comments on Castelijns and van den Brekel: imaging of lymphadenopathy in the neck. *European Journal of Radiology*. 2003;13: 2236
30. H. Rowley, E. Grant, T. Roberts. Diffusion MR imaging theory and application. *Clinical Neuroimaging*. 1999;9: 343-61.
31. A.M. Herneth, S. Guccione, M. Bednarski. Apparent diffusion coefficient: a quantitative parameter for in vivo tumor characterization. *European Journal of Radiology*. 2003; 45: 208-13.
32. R. Sigal, T. Vogl, J. Casselman, G. Moulin, F. Veillon, R. Hermans, F. Dubrulle, et al. Lymph node metastases from head and neck squamous cell carcinoma: MR imaging with ultrasmall superparamagnetic iron oxide particles (Sinerem MR)—results of a phase-III multicenter clinical trial. *European Journal of Radiology*. 2002;12: 1104-13.
33. Guo Y, Cai Y. Q, Cai Z. L. Differentiation of clinically benign and malignant breast lesions using diffusion-weighted imaging. *J Magn Reson Imaging* 2002; 16:172–78.

34. Gauvain KM, McKinstry RC, Mukherjee P. Evaluating pediatric brain tumor cellularity with diffusion-tensor imaging. *American Journal of Radiology*. 2001; 177:449–54.
35. Sugahara T, Korogi Y, Kochi M, et al. Usefulness of diffusion-weighted MRI with echo-planar technique in the evaluation of cellularity in gliomas. *J MagnReson Imaging*. 1999; 9:53–60.
36. Lang P, Wendland MF, Saeed M, et al. Osteogenic sarcoma: noninvasive in vivo assessment of tumor necrosis with diffusion-weighted MR imaging. *Radiology* 1998; 206:227–35.
37. Neil JJ. Measurement of water motion (apparent diffusion) in biological systems. *Concepts MagnReson* 1997; 9: 385–401.
38. Moffat B.A, Chenevert T.L, Lawrence T.S. Functional diffusion map: a noninvasive MRI biomarker for early stratification of clinical brain tumor response. *Proc Natl Acad Sci U S A* 2005; 102:5524–29.
39. Thoeny HC, De Keyser F, Chen F. Diffusion weighted MR imaging in monitoring the effect of a vascular targeting agent on rhabdomyosarcoma in rats. *Radiology* 2005; 234:756–64.
40. Pérez Y, Lahrech H, Miquel C, Barnadas R, Sabés M, Rémy C et al. Measurement by Nuclear Magnetic Resonance Diffusion of the Dimensions of the Mobile Lipid Compartment in C6 Cells. *American Association for Cancer Research. H* 2002; 62: 5672–77.
41. Abish Y. G, Roshdy H. M and Eniate M. A. Benign versus malignant cervical lymph nodes: Differentiation by Diffusion Weighted MRI. *AAMJ*. 2011; 9(3):2.

42. ElSaid N. A. E, Nada O. M. M, Habib Y. S, Semeisem A.R, Khalifa N.M. Diagnostic accuracy of diffusion weighted MRI in cervical lymphadenopathy cases correlated with pathology results. *The Egyptian Journal of Radiology and Nuclear Medicine* 2014; 45 (4): 1115-25.
43. Choure A. A, Khaladkar S. M, Jain S. Differentiation of benign and malignant cervical lymph nodes on MRI with special emphasis on DWI. *International Journal of Radiology and Diagnostic Imaging* 2019; 2(2): 96-105.
44. Essig H, Warraich R, Zulfiqar G, Rana M, Eckardt AM, Gellrich NC et al. Assessment of cervical lymph node metastasis for therapeutic decision-making in squamous cell carcinoma of buccal mucosa: a prospective clinical analysis. *World Journal of Surgical Oncology*. 2012; 10(1):253.
45. Curtin HD, Ishwaran H, Mancuso AA, Dalley RW, Caudry DJ, McNeil BJ. Comparison of CT and MR imaging in staging of neck metastases. *Radiology* 1998; 207:123–130.
46. E.A. Eisenhauer, P. Therasse, J. Bogaerts, L.H. Schwartz, D. Sargent, R. Ford et al. New response evaluation criteria in solid tumours: Revised RECIST guideline (version 1.1). *European Journal of Cancer* 2009; 45: 228 – 47.
47. Y. Zhang, J. Chen, J. Shen, J. Zhong, R. Ye, B. Liang. Apparent diffusion coefficient values of necrotic and solid portion of lymph nodes: Differential diagnostic value in cervical lymphadenopathy. *Clinical Radiology* 2013; 68: 224-31.

**ANNEXURE I
INFORMED CONSENT**

TITLE OF THE STUDY: “COMPARISON OF DIAGNOSTIC ROLE OF DIFFUSION WEIGHTED IMAGING (DWI) IN THE DIFFERENTIATION OF BENIGN AND MALIGNANT CERVICAL GROUP OF LYMPH NODES WITH PATHOLOGICAL CORRELATION- A ONE YEAR OBSERVATIONAL STUDY AT KLES DR PRABHAKAR KORE HOSPITAL AND MRC, BELAGAVI”

PRINCIPAL INVESTIGATOR: REG. NO. BS0118004

INTRODUCTION AND PURPOSE:

Lymphadenopathy is defined as an abnormal increase in size and / or alteration in consistency of the lymph nodes. DWI is a non invasive procedure which helps in differentiating the cervical group of malignant lymph nodes from the benign ones. The characterization is based on the size, alteration in shape, architecture, difference in signal intensities picked up on the different sequences of MRI and the ADC values in the ROI.

PROCEDURE:

I request you to kindly participate in the study titled “COMPARISON OF DIAGNOSTIC ROLE OF DIFFUSION WEIGHTED –MR IMAGING IN THE DIFFERENTIATION OF BENIGN AND MALIGNANT CERVICAL GROUP OF LYMPH NODES WITH PATHOLOGICAL CORRELATION – A ONE YEAR HOSPITAL BASED OBSERVATIONAL STUDY at Dr. Prabhakar Kore charitable hospital and Medical Research Centre, Belagavi” conducted by REG.NO. BS0118004, post graduate in Radiodiagnosis at J. N. Medical College Belagavi,

Karnataka, under the guidance of Dr. _____, HOD Dept. of Radiodiagnosis, J. N. Medical College, Belagavi. During the study, you will be asked questions regarding your present and past medical history and you will be required to answer to the best of your knowledge. You will also be asked to produce your histopathological reports as per the requirements of the study design.

If you agree to participate in the study, please furnish the necessary details pertaining to the study.

BENEFITS:

- Noninvasive modality.
- Less time needed for reporting when compared to the pathological analysis.

DISADVANTAGES:

- Patient compliance throughout the scan.
- Patients with known contraindications for MRI scan, cannot undergo the scan.

COMPLICATIONS:

- No risk to the patient has been documented from MR imaging of the brain and neck conducted earlier.

ALTERNATIVES:

If patient refuses to take part in the study, his / her treatment or any other further investigations the patient wants to undergo, in future, in KLE will not be affected by his / her decision.

VOLUNTARY PARTICIPATION/WITHDRAWAL:

Taking part in this study is voluntary. The patient may choose not to take part in this study, or if they decide to take part, they can later change their mind and withdraw from the study anytime. Their decision will not change the present or future health care or other services that they would receive.

COSTS: NIL (The study will be conducted on the patients who are referred for MRI scan to the Department of Radiology, KLES Dr Prabhakar Kore Hospital And MRC, by their referring consultants to plan the further management of the case and hence the patient will bear the charges for the scan).

Payment for Participation: No incentive will be paid to the subjects for participating in the study.

COMPENSATION:

If the patient sustains any injury/ illness during the scan, treatment whatever available at KLES Dr Prabhakar Kore Hospital And MRC, Belagavi, will be offered to them. No reimbursement or compensation will be given.

CONFIDENTIALITY: the necessary information collected about the patient during the course of the study will be kept confidential to the extent permitted by the law. The patient IP/OP numbers will identify them in this research records. Information from this study may be published but the patient identity will be kept confidential in any of the publications.

QUESTION:

If any enquiries in the future or in case of research related injury/illness, the patient may contact the following person.

REG. NO. BS0118004	Dr _____	Dr. Roopa M Bellad
Post-Graduate, Department of Radio-Diagnosis. J.N.Medical College, Belagavi	Guide , Professor and Head, Department Of Radio- Diagnosis J.N.Medical College Belagavi	Professor and Unit Head Of Pediatrics Chairman, J.N. Medical College Institutional Ethical Committee for Human Subjects Research

CONSENT TO PARTICIPATE IN RESEARCH STUDY:

1. I understand that I am participating in the study, which includes Magnetic Resonance Imaging of brain and neck.
2. I confirm that I have read and understood the information in the patient information sheet. I have been explained the procedure in detail along with information about the advantages and disadvantages of taking part in the study. I have been given the opportunity to discuss all aspects of the trial, to ask questions and hereby consent to participation in the trial outlined above.
3. I understand that the decision to take part in this study is completely voluntary and I am aware that I can choose to withdraw from the study at any point of time.
4. I consent to the photographing or recording of the procedure to be performed including appropriate portions of my body, for medical, scientific or educational purposes provided my identity is not revealed in the pictures or by the descriptive texts accompanying them.
5. I understand that there is no significant risk involved in the test that would be done in this study.
6. No guarantee or assurance has given by anyone as to the results that may be obtained.
7. My signature on this form signifies that I have willingly decided to participate after understanding the above information.

Participant's Name/ legally authorized representative _____

Signature _____

Name and signature of witness _____

Name and signature of interviewer _____

ANNEXURE II – ETHICAL CLEARANCE LETTER



K.L.E. ACADEMY OF HIGHER EDUCATION AND RESEARCH
(Decmod – to-be- University)

Accredited 'A' Grade by NAAC (2nd Cycle)

Placed in Category 'A' by MHRD (GoI)

JAWAHARLAL NEHRU MEDICAL COLLEGE,
NEHRU NAGAR, BELAGAVI-590010 (KARNATAKA-INDIA)

Website: <http://www.jnmc.edu>
E-Mail : dome@jnmc.edu

Phone: (+ 91-(0)831 Office : 2472550
Principal: 2471701
Fax No. +91 (0)831 – 2470759

Ref: MDC/DOME/15

Date: 24/11/2018

To,

REG. NO. BS0118004

PG student in Radio-Diagnosis,
J.N.Medical College,
BELAGAVI.

Sub: Institutional Ethical Clearance for the study.

With reference to the above, we wish to inform you that your proposed research project titled "COMPARISON OF DIAGNOSTIC ROLE OF DIFFUSION WEIGHTED IMAGING (DWI) IN THE DIFFERENTIATION OF BENIGN AND MALIGNANT CERVICAL GROUP LYMPH NODES WITH PATHOLOGICAL CORRELATION – A ONE YEAR OBSERVATIONAL STUDY AT KLES DR PRABHAKAR KORE HOSPITAL AND MRC, BELAGAVI", is ethical and justifiable. The proposed research project has been cleared by the JNMC Institutional Ethics Committee on Human Subjects Research.

(Dr. Arathi Darshan)
Member Secretary
JNMC Institutional Ethics Committee
on Human Subjects Research,
J.N.Medical College, Belagavi.

(Dr. Roopa M Bellad)
Chairman,
JNMC Institutional Ethics Committee
on Human Subjects Research,
J.N.Medical College, Belagavi.

ANNEXURE III - STUDY PROFORMA

PROFORMA FOR DATA COLLECTION

NAME _____

DATE _____

AGE/ SEX _____ / _____

ADDRESS _____

MRI NUMBER: _____

CHIEF COMPLAINTS:

HISTORY OF PRESENTING ILLNESS:

PAST HISTORY:

FAMILY HISTORY:

**TREATMENT HISTORY- CHEMOTHERAPY/RADIOTHERAPY (IF
TAKEN):**

OPERATIVE HISTORY (IF ANY):

**HISTOPATHOLOGY/ CYTOLOGY/ BIOPSY REPORT OF THE
RESECTED LYMPH NODES:**

ANNEXURES IV - FIGURES

CASE 1- REACTIVE LYMPHADENITIS



A

B

Figure 8-A and B: T2 WI coronal (A) and sagittal (B) fat suppressed images show multiple subcentimetric bilateral level II and left level III and IV nodes.



C

D

Figure 8- C and D: DWI (C) and ADC (D) axial images show few well defined subcentimetric nodes in the bilateral level II and II with no diffusion restriction.

CASE 2: CASE OF SQUAMOUS CELL CARCINOMA OF TONGUE WITH METASTASIS TO BILATERAL LEVEL IB AND BILATERAL LEVEL II.

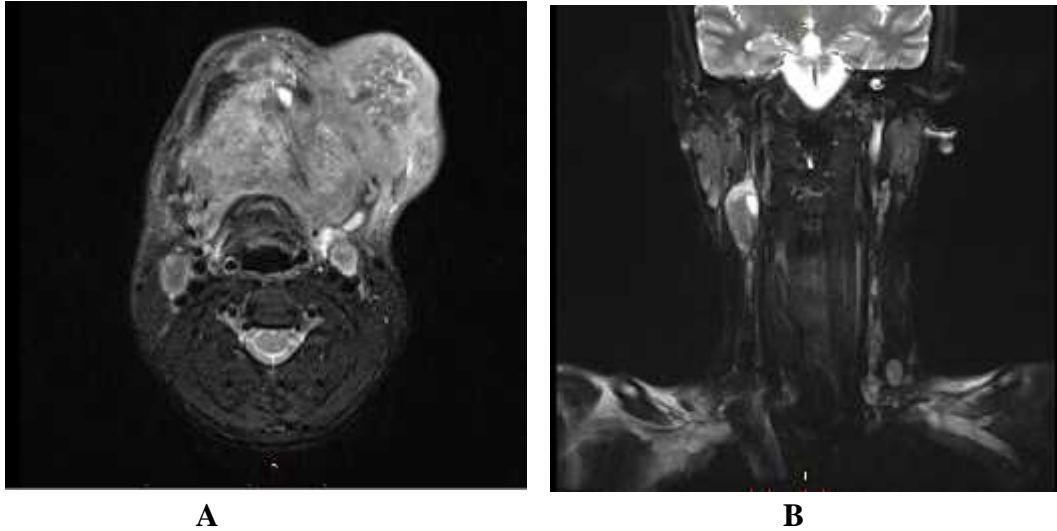


Figure 9-A: T2 WI axial images showing large fairly well defined exophytic heterogeneously hyperintense mass lesion with irregular margins in the tongue extending into the oral cavity, breaching the skin and protruding outwards.

Figure 9-B: T2WI coronal image shows an enlarged right Level II node with loss of fatty hilum.

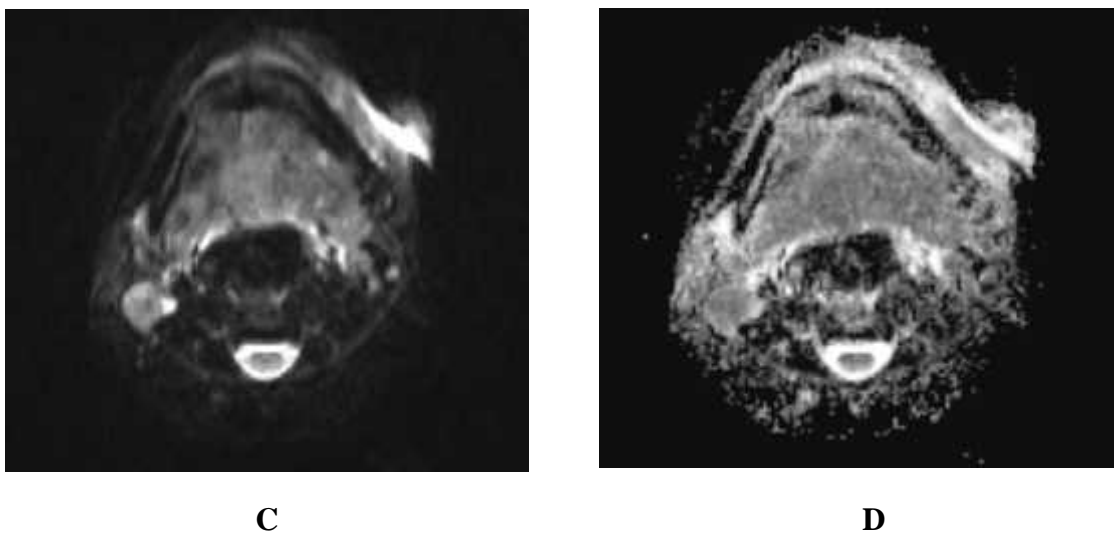


Figure 9-C: DWI at b 800- shows restriction Figure 9-D: ADC shows ofright Level II enlarged nodecorresponding low signals.

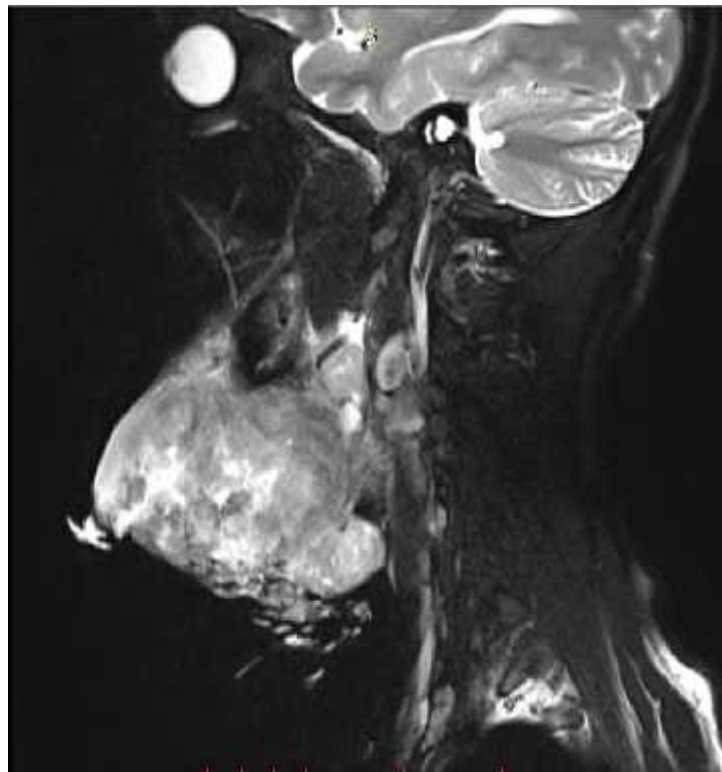
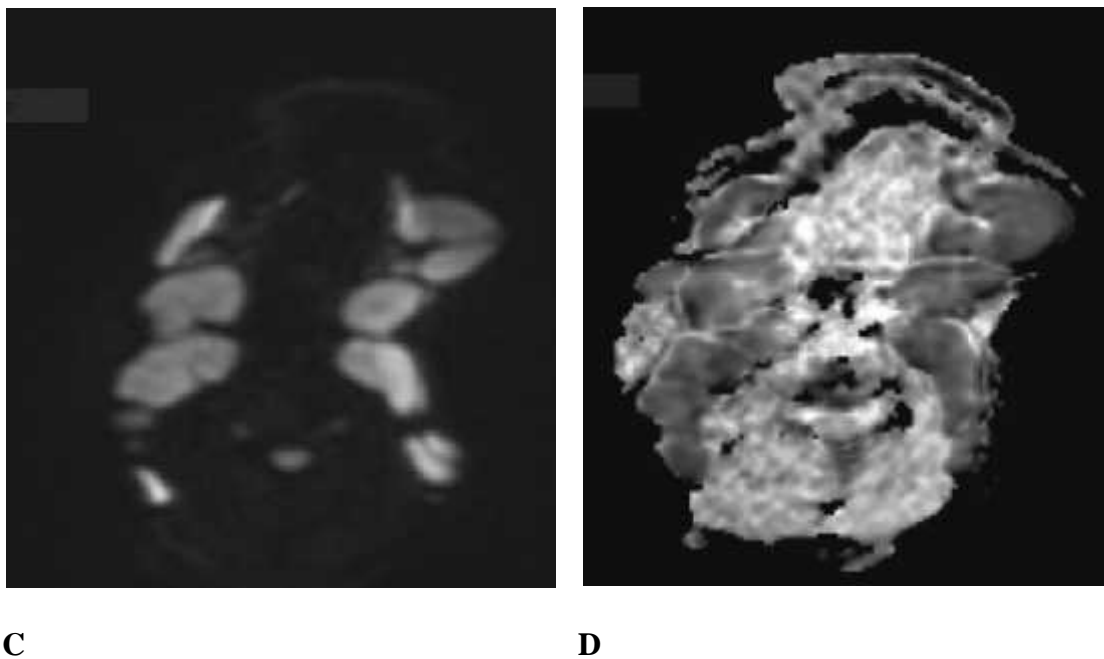
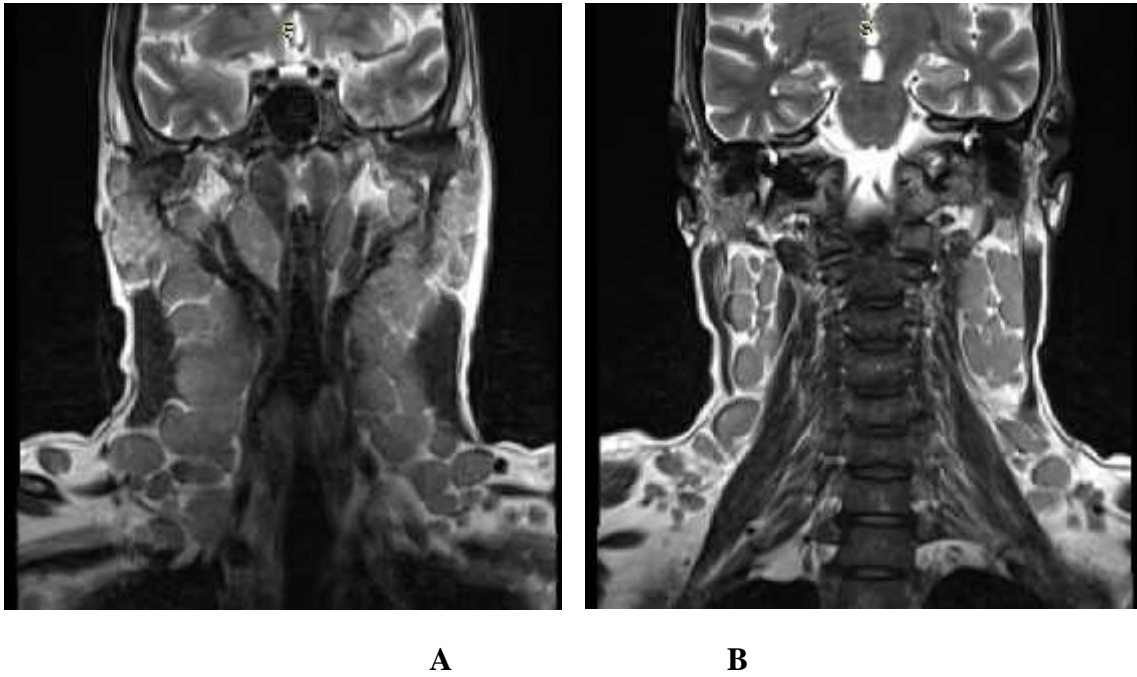


Figure 9-E: T2WI left para-sagittal image shows a large T2 heterogeneously hyperintense mass lesion in the oral cavity with multiple left level II, III and IV lymph nodes.

CASE 3: NON-HODGKIN LYMPHOMA



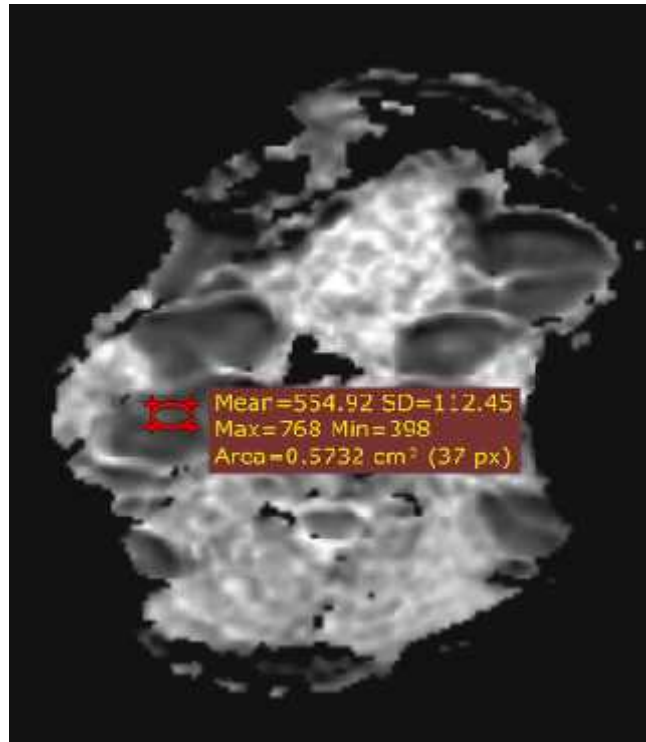
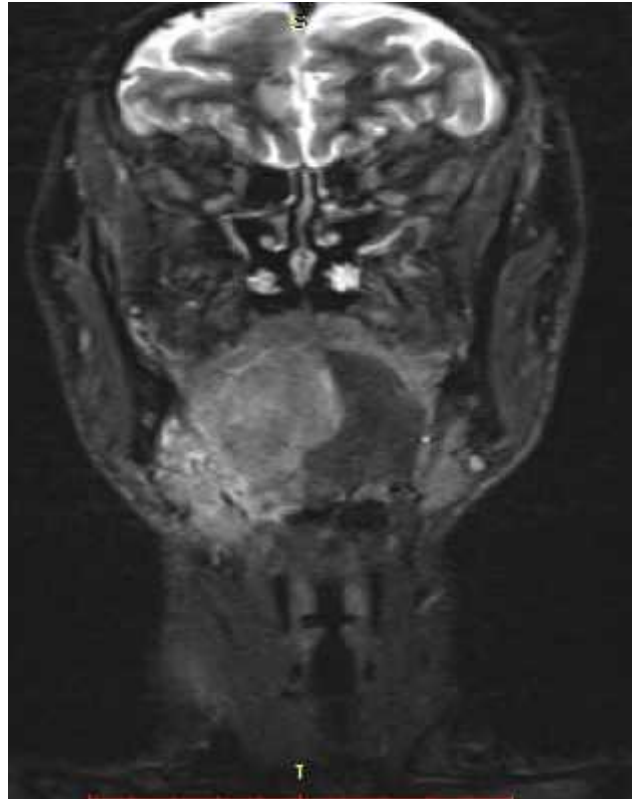


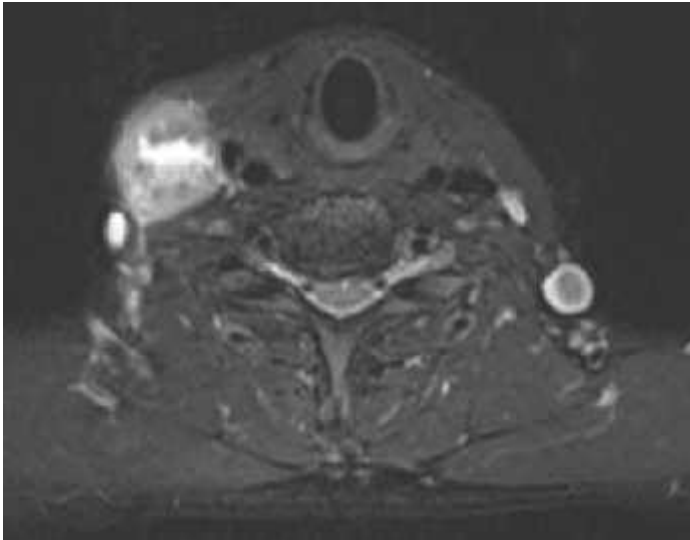
Figure 10- E:ADC value of one of the node showing value of $554.92 \times 10^{-6} \text{ cm}^2/\text{min}$.

CASE 4: SQUAMOUS CELL CARCINOMA OF TONGUE WITH WITH LYMPH NODE METASTASES TO RIGHT LEVEL IB AND RIGHT LEVEL III WITH NECROTIC COMPONENTS AND EXTRACAPSULAR EXTENSION.



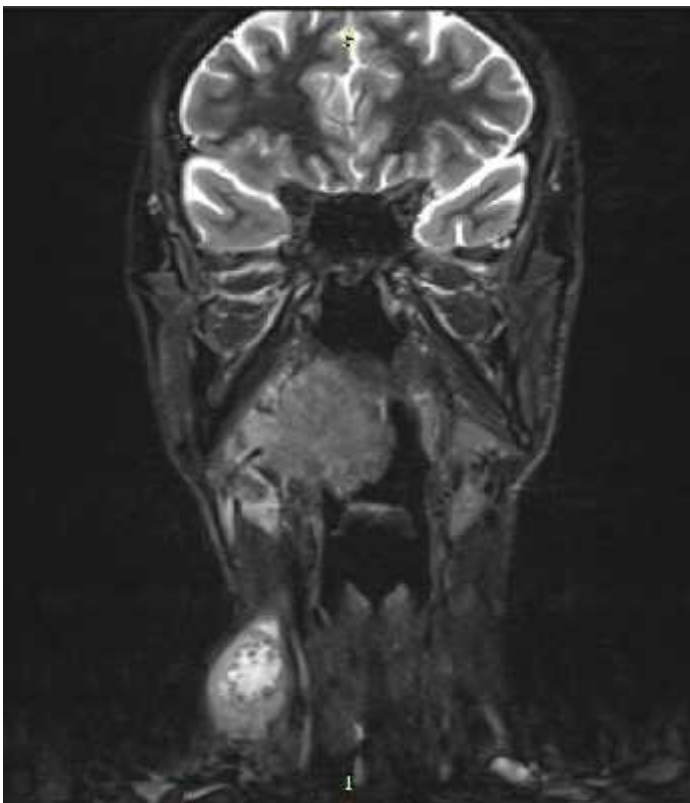
A

Figure 11-A: T2WI coronal image showing hyperintense mass lesion in the tongue extending upto the submandibular space.



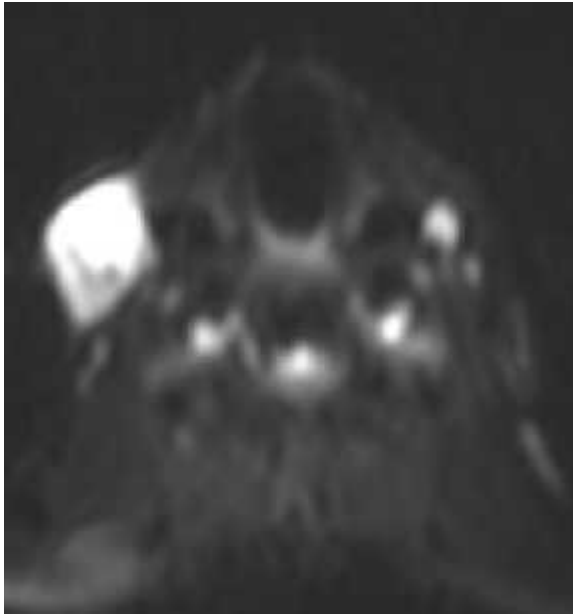
B

Figure 11- B: T2 axial image showing heterogeneously hyperintense enlarged necrotic lymph node in right level III.

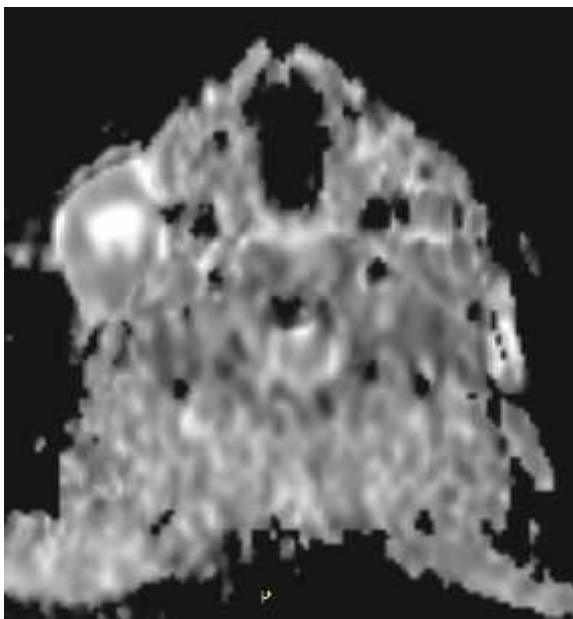


C

Figure 11- C: T2 coronal image showing an enlarged right level III lymph nodes with central T2 hyperintense necrotic core and irregular margins suggestive of metastatic necrotic node with extracapsular extension.



D



E

Figure 11- D and E:DWI shows diffusion restriction in the solid portion with central area showing high signal intensity on both DWI and ADC suggestive of necrotic component.

CASE 5: K/C/O CARCINOMA OF RIGHT BUCCAL MUCOSA WITH 3 RIGHT LEVEL IB LYMPH NODES SHOWING METASTASES WITH EXTRACAPSULAR EXTENSION.

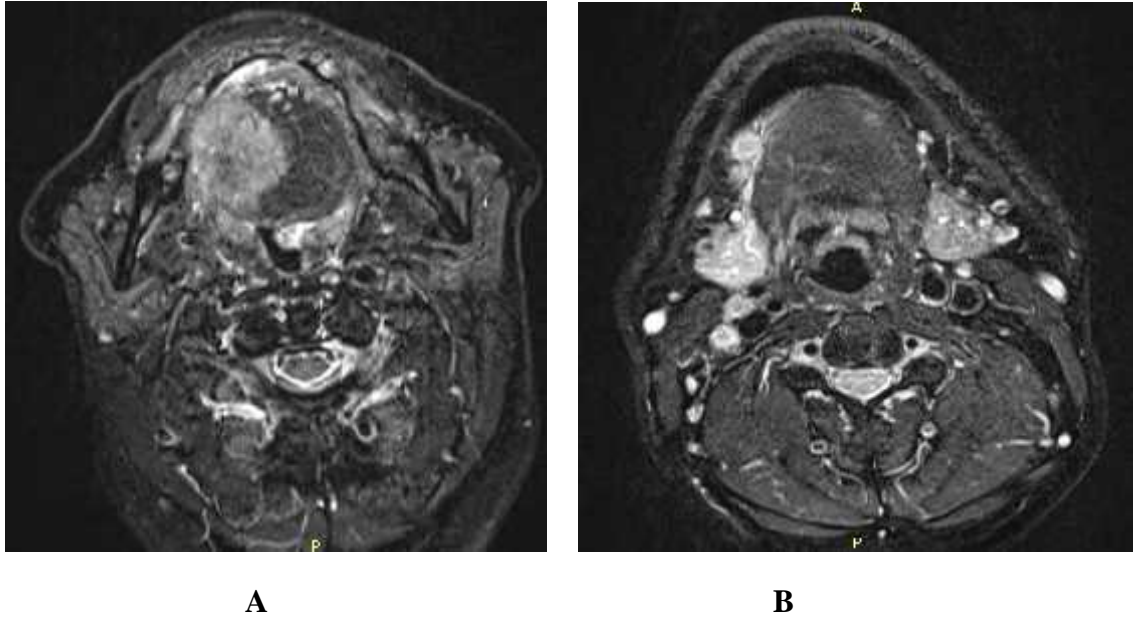


Figure 12- A and B: T2 TIRM axial images showing well defined hyperintense lesion in the right lateral aspect of the tongue with two subcentimetric lymph nodes with ill defined margins in the right level II suggestive of extrasapsular spread.

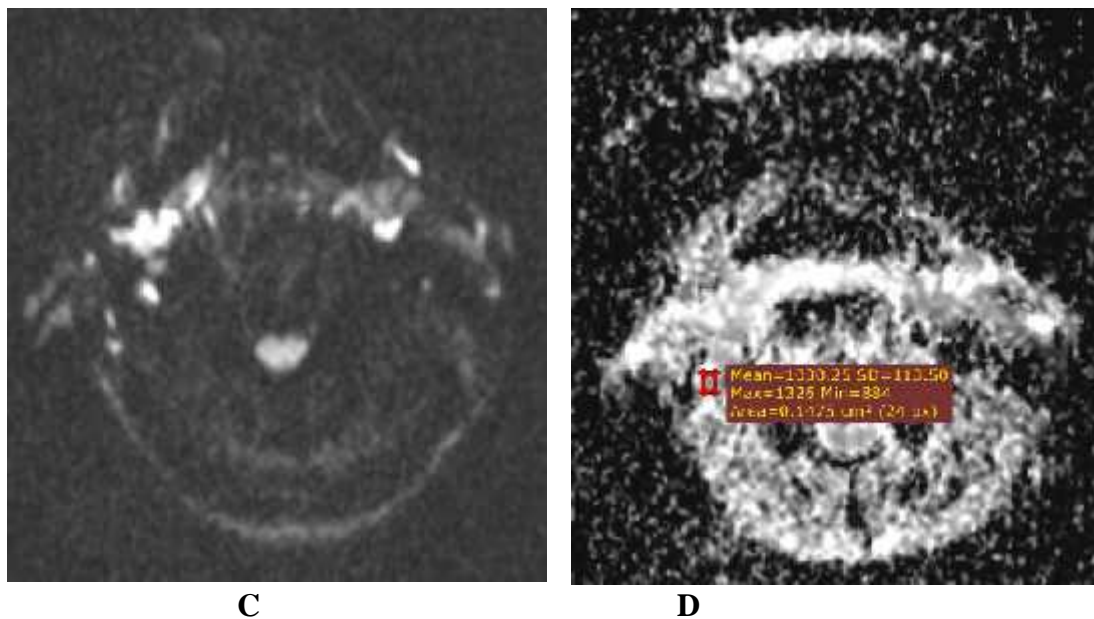
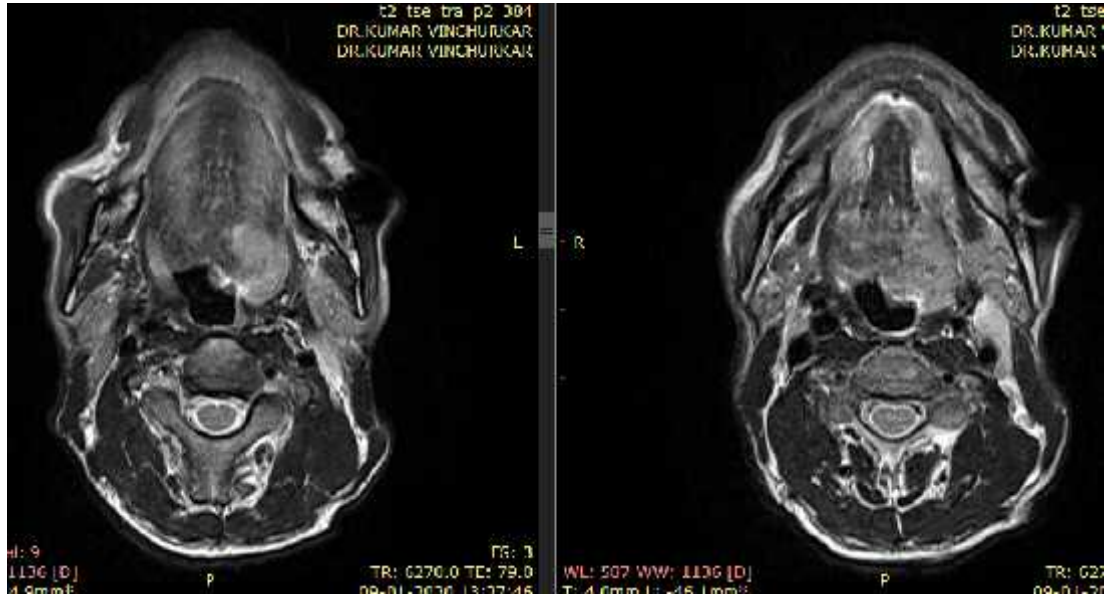


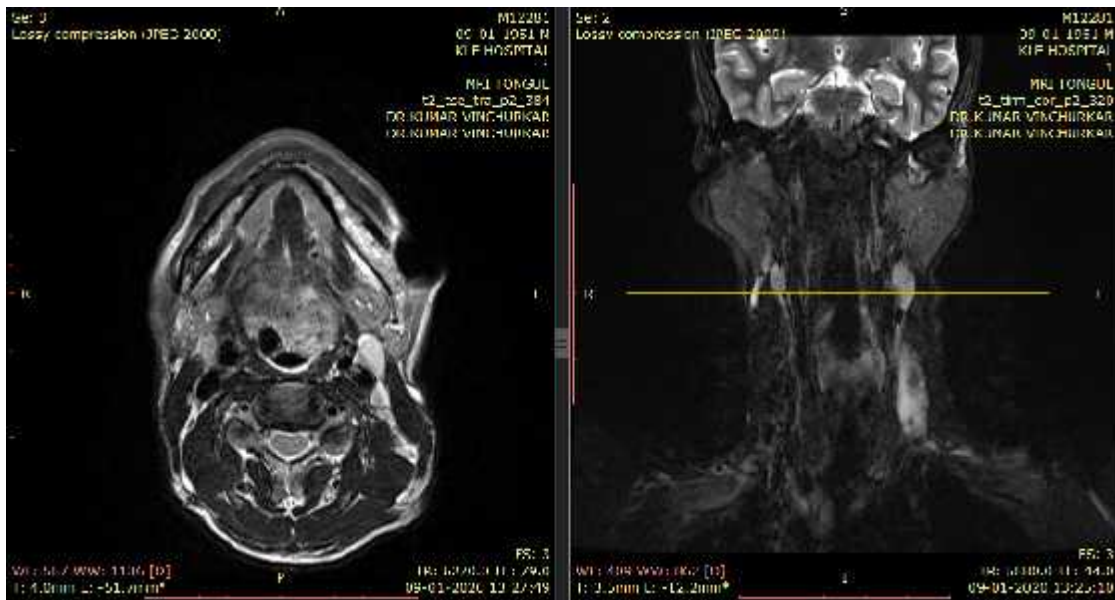
Figure 12- C and D: On DWI, diffusion restriction seen in the subcentimetric right level Ib nodes with ADC value of $1030.25 \times 10^{-6} \text{ cm}^2/\text{min}$.

CASE 6: SQUAMOUS CELL CARCINOMA OF TONGUE WITH METASTASIS TO LEFT LEVEL IIA NODE.



A

Figure 13-A: T2 axial images showing hyperintense mass lesion in the base of tongue on left lateral aspect and reaching upto the midline.



B

Figure 13-B: T2 axial and coronal image shows marginally enlarged lymph node in the left level IIA group.

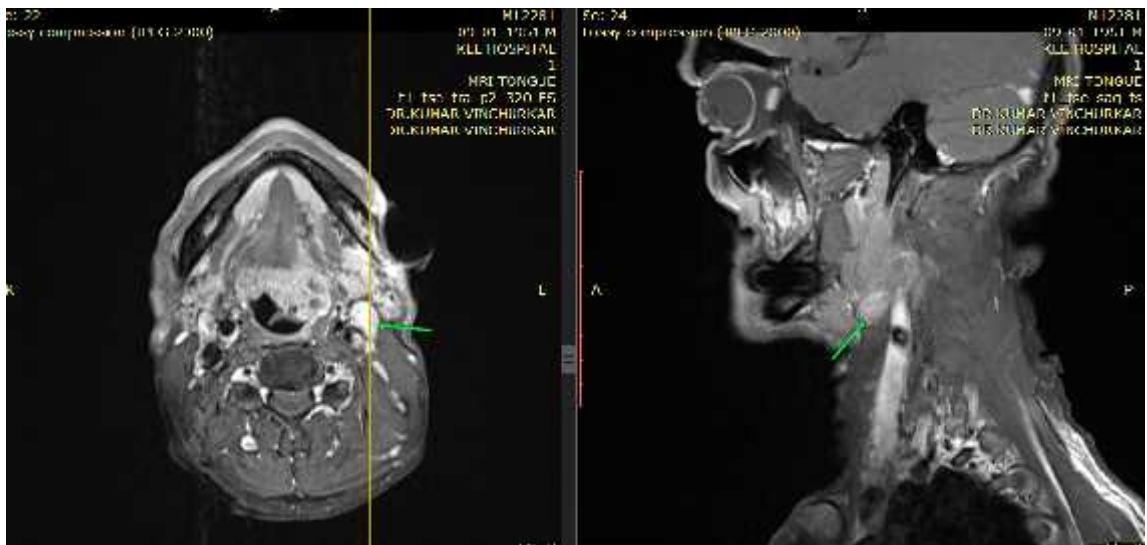
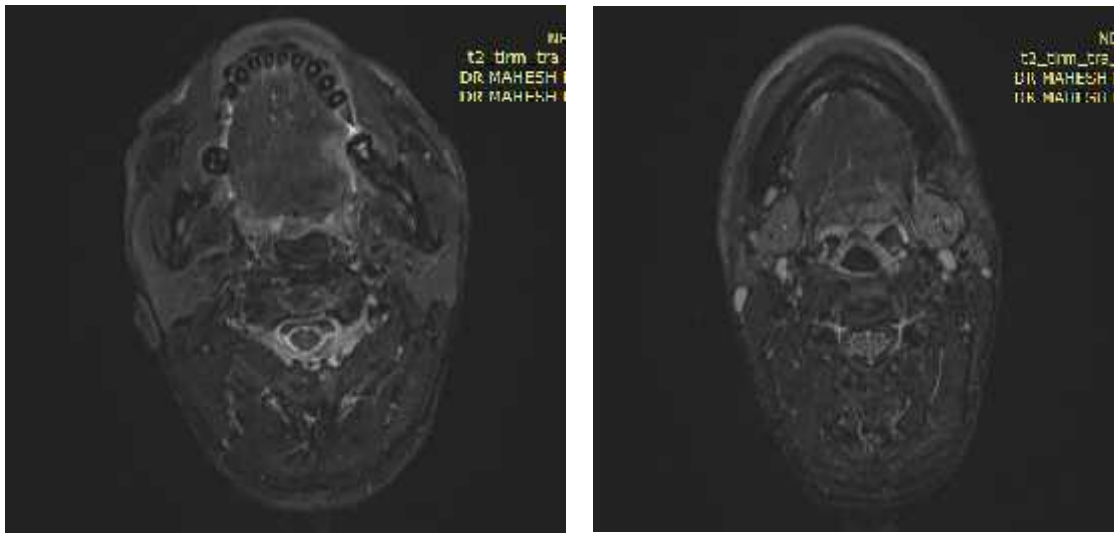


Figure 13-E: On post gadolinium (contrast) - axial and sagittal T1 W fat suppression images, heterogeneously enhancing left level IIa node with loss of fatty hilum.

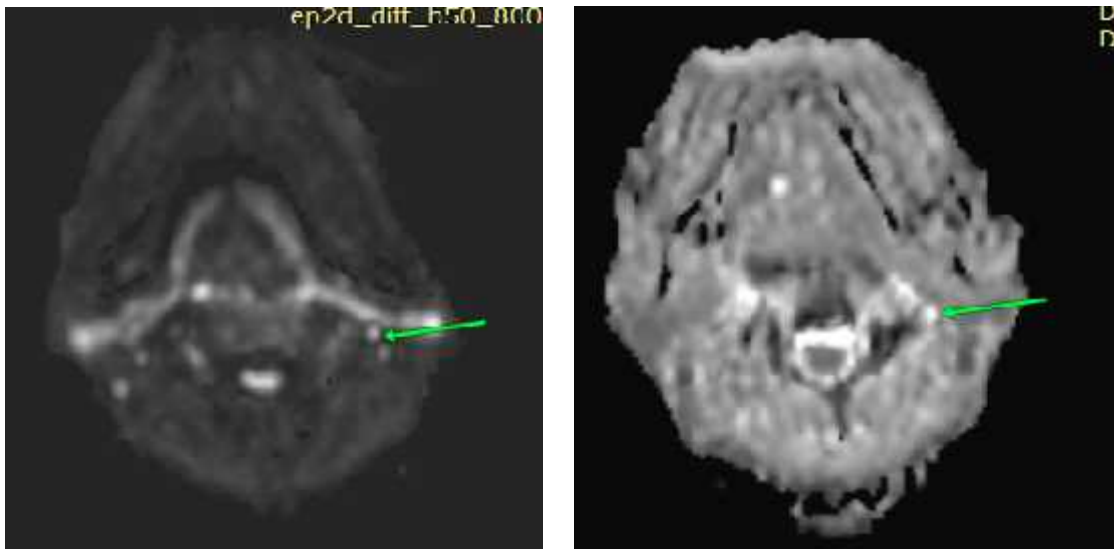
CASE 7: SQUAMOUS CELL CARCINOMA OF TONGUE WITH NO NODAL METASTASIS.



A

B

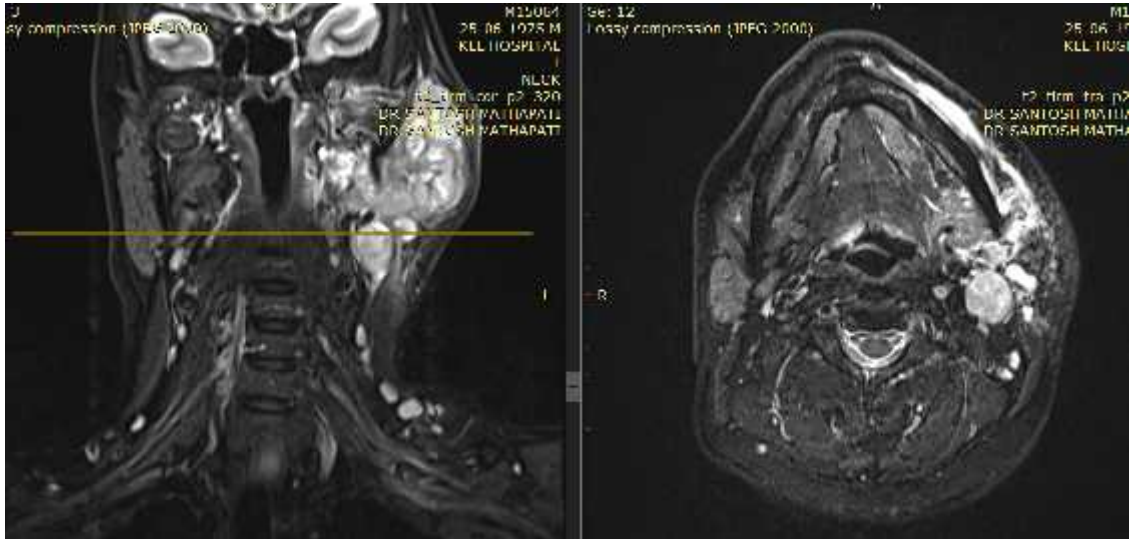
Figure 13- A and B: T2 axial images, (A and B)- showing hyperintense mass lesion in the left lateral aspect of the tongue and few subcentimetric nodes in the right level IB and bilateral IIA.



CD

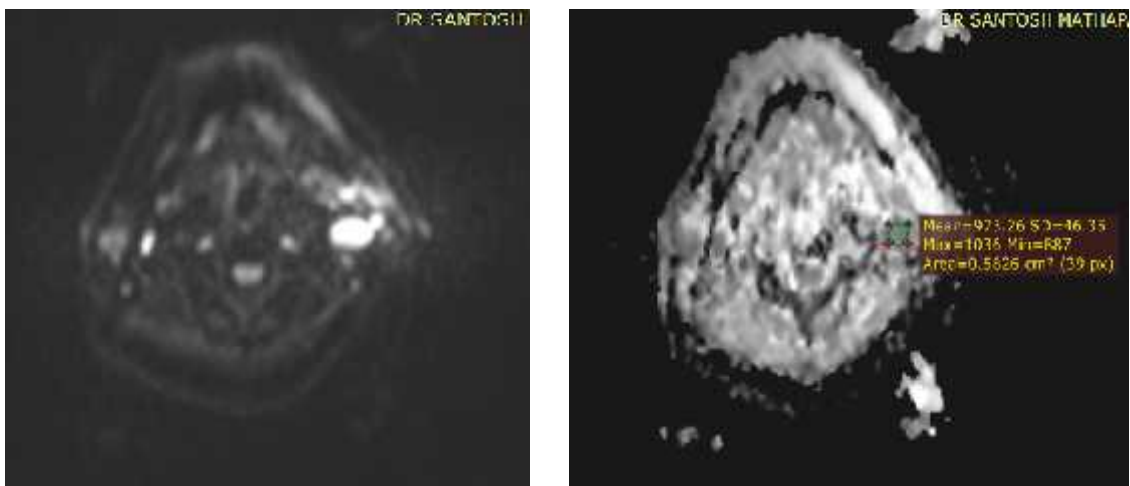
Figure 13- C and D: DWI (b- 800)and ADC show a subcentimetric left level II node with no diffusion restriction.

CASE 8: MUCOEPIDERMOID CARCINOMA OF LEFT PAROTID GLAND WITH METASTASES TO LEFT LEVEL Ib AND IIa LYMPH NODES.



A

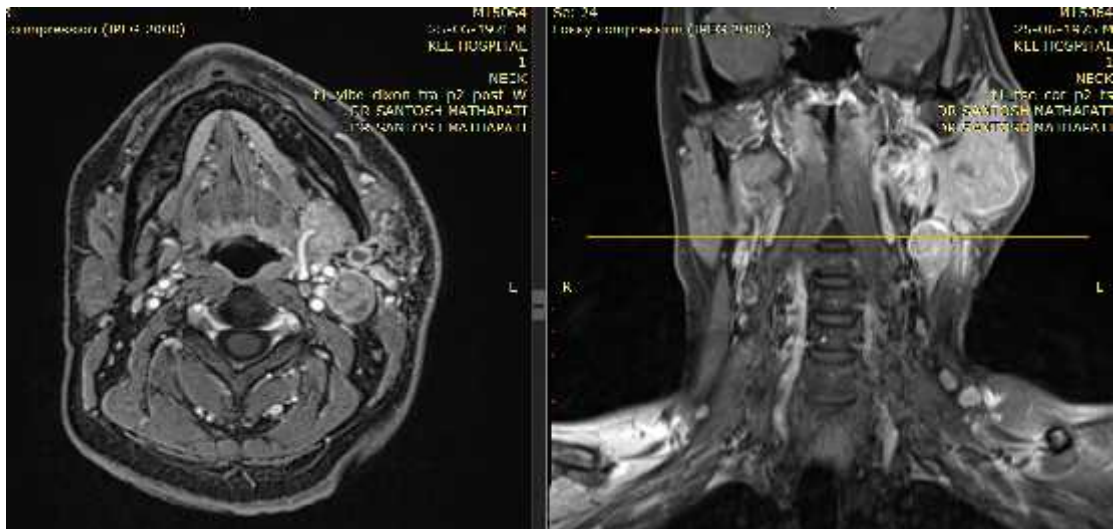
Figure 14-A: T2 coronal and axial T2 Fat suppressed image of neck showing diffuse enlargement of left parotid gland with heterogeneously hyperintense mass lesion. Multiple subcentimetric bilateral level Ib, II, III and IVa nodes. An enlarged rounded left level Ib node noted with loss of fatty hilum.



B

C

Figure 14-B and C: DWI (b - 800) and ADC axial images of neck showing diffusion restriction in the left level II node suggestive of metastasis.



D

Figure 14-D: T2 axial and coronal T1 fat suppressed post contrast images showing heterogeneously enhancing mass lesion in the left parotid gland involving both the superficial and deep lobe with heterogeneously enhancing lymph nodes in the left level Ib and II suggestive of metastases.

KEY TO MASTERSHEET

Variable	Code	Value
SHAPE	0	Oval
	1	Round
Margins	0	Well defined
	1	Ill defined
Necrosis	0	Absent
	1	Present
Fatty hilum	0	Maintained
	1	Loss of fatty hilum
Short axis	0	Subcentimetric
	1	Enlarged
DWI	0	No Restriction
	1	Shows restriction
Study diagnosis	0	Benign
	1	Malignant
FNAC/histopathology diagnosis	0	Benign
	1	Malignant

SR NO	MRI NO	AGE	SEX	PRESENTING ILLNESS	LEVELS OF THE LYMPH NODES INVOLVED	LEVEL	FEATURES OF SUSPICIOUS CERVICAL LYMPH NODES								FNAC REPORTS OF LYMPH NODES	HPR REPORTS	Study diagnosis	Final diagnosis	
							SIZE	SHAPE	MARGINS	NECROSIS	FATTY HILUM	SHORT AXIS	L/S RATIO	DWI					ADC VALUE
1	9537	11	F	c/o fever and swelling in the neck on left side	bilateral level Ib, II, III	right level II	1.9 x 1.3 cms	0	0	0	0	1	1.4	1	1253.35	NA	Left second branchial cyst with Inflammatory cervical lymphadenopathy	0	0
2	10038	66	F	c/o fever and swelling in neck on left side	Bilateral level Ib, II, III, IV and V	left level V	3.2 x 2.8 cms	0	0	1	1	1	1.1	1	1342.24	Inflammatory granulomatous disease- tuberculosis etiology with necrotic component	NA	0	0
3	14256	43	M	c/o small swelling on the lateral aspect of tongue on right side	Right level II, III and IV	right level II	1.0 x 0.6 cms	0	0	0	0	0	1.6	1	1250.52	NA	squamous cell carcinoma of tongue with no metastatic cervical lymphadenopathy	0	0
4	12456	14	F	c/o fever with cervical lymphadenopathy	Bilateral level Ib, II, III, IV and V	right level II	1.6 X 1.1 cms	0	0	1	0	1	1.4	0	1181.65	Reactive lymphadenitis	NA	0	0
5	16546	24	M	k/c/o carcinoma of right buccal mucosa	Right level II, III and IV	Right level Ib	2.0 x 1.3 cms	0	1	0	1	1	1.5	0	1026.93	Metastatic lymphadenopathy	3 Right level Ib lymph nodes shows metastasis with extracapsular extension	0	1
6	15206	68	M	c/o swelling and pain in the right cheek region	Right level Ib, and II	Right level IB	2.0 x 1.0 cms	1	0	0	1	1	2	1	910.28	NA	Moderately differentiated squamous cell carcinoma with metastasis to right level Ib and II cervical lymph nodes	1	1
7	14590	24	F	c/o swelling in the tongue	right level IVb	right level IVb	1.5 x 1.3 cms	0	0	0	0	1	1.1	0	1145.27	Hemangioma of tongue with lymph nodes showing benign features	NA	0	0
8	12345	56	M	c/o neck pain with fever	Bilateral level II and III	right level II	3.2 x 1.2 cm	0	0	0	0	1	2.6	0	1136.56	Reactive lymphadenitis	NA	0	0
9	13189	54	M	c/o hoarseness of voice	level Ia, bilateral level II, III & IV	right level II	1.8 x 1.1 cms	1	1	0	1	1	1.6	1	806.63	Metastatic right level II lymph nodes	Poorly differentiated squamous cell carcinoma of vocal cords with metastasis to bilateral level Ib lymph nodes	1	1
10	14995	56	M	c/o bilateral cervical lymphadenopathy	level IA , bilateral level Ib, II & III	right level Ib	1.4 x 0.6 cm	0	0	0	0	0	2.3	0	1149.46	Reactive lymphadenitis	NA	0	0
11	14284	76	M	k/c/o carcinoma right buccal mucosa- post operative and chemotherapy status, for follow -up	level Ia, bilateral level II, III & IV	right level II	1.1 x 0.5 cms	0	0	0	0	0	2.2	1	881.23	NA	squamous cell carcinoma of righ buccal mucosa with two of right level Ib lymph nodes showing metastases	1	1
12	14299	57	M	c/o ulcerative growth on the right lateral aspect of the tongue	IA, bilateral level IB	left level Ib	1.6 x 0.9 cms	1	1	0	0	0	1.7	1	628.28	NA	poorly differentiated squamous cell carcinoma with metastasis to bilateral level Ib lymph nodes	1	1
13	17677	78	F	c/o neck pain on left side	level Ia, bilateral level Ib, II, III & V	left level V	1.3 x 0.8 cms	0	0	0	0	0	1.6	1	822.76	reactive lymph node	NA	1	0
14	14760	67	F	c/o carcinoma tongue	level II and III	Left level II	1.2 x 0.5 cm	0	0	0	0	0	2.4	0	1135.73	NA	squamous cell carcinoma of tongue with no lymph nodal metastases	0	0
15	13456	49	F	c/o neck in pain since 4 days	level Ia, bilateral level Ib, II and III	right level Ib	1.3 x 0.6 cms	0	0	0	0	0	2.1	0	1211.23	NA	squamous cell carcinoma of tongue with no nodal metastases	0	0
16	13047	67	F	c/o carcinoma tongue	right level II, III & IV	right level II	3.1 x 2.7 cms	1	0	1	1	1	1.1	0	1420.26	necrotic right level II	poorly differentiated squamous cell carcinoma with metastasis to right level II and III	0	1
17	14567	86	M	c/o carcinoma tongue	IA, bilateral level Ib, II	right level Ib	1.1 x 0.9 cms	1	1	0	1	0	1.2	1	656.78	metastatic right level Ib	squamous cell carcinoma of tongue with lymph node metastases to bilateral level Ib	1	1
18	13456	68	F	c/o ulcerative lesion on the tongue	bilateral level Ib	right level Ib	1.2 x 0.8 cms	0	0	0	0	0	1.5	0	1211.13	NA	squamous cell carcinoma of tongue with no lymph nodal metastases	0	0
19	12550	47	F	c/o swelling in the tongue	bilateral level Ib, II & III	left level IB	1.2 x 0.7 cms	0	0	0	0	0	1.7	1	1178.34	NA	squamous cell carcinoma of tongue with no lymph nodal metastases	0	0
20	23456	52	M	c/o swelling and pain in the tongue and floor of mouth	bilateral level IB, II and V	left level II	3.5 x 1.5 cm	0	0	0	0	1	2.3	1	776.76	NA	squamous cell carcinoma of the tongue with metastases to left level Ib and II	1	1
21	12281	91	M	c/o ulcerative growth in tongue with cervical lymphadenopathy	left level IIb	left level IIb	2.1 x 1.1 cms	0	0	0	0	1	1.9	1	998.02	NA	squamous cell carcinoma of the tongue with left level IIa node showing metastasis	1	1
22	24356	25	M	c/o swelling in the right preauricular region	Right level Ib	right level Ib	1.5 x 0.7 cms	0	0	0	0	0	2.1	0	1244.34	NA	pleomorphic adenoma of parotid gland with no metastasis	0	0
23	13425	54	M	c/o tongue lesion on the left lateral aspect	bilateral level Ib, left II and III	left level Ib	1.8 x 0.8 cms	0	0	0	0	0	2.2	0	1189.78	NA	squamous cell carcinoma of tongue with no nodal metastasis	0	0

25	3327	34	M	c/o lesion in the right buccal mucosa	bilateral level Ib, II and right level III	right level Ib	2.2 x 1.0 cms	0	0	0	0	1	2.2	1	1045.35	NA	left buccal mucosa carcinoma with no lymph node metastases	0	0
26	12795	76	M	c/o lesion in the tongue with cervical lymphadenopathy	Bilateral level Ib, II, III, IV and V	right level II	1.5 x 1.5 cms	1	1	0	1	1	1	1	957.53	right level II lymph node positive for malignant cells	squamous cell carcinoma of tongue with metastases to bilateral level II and IVa nodes	1	1
27	13723	36	M	c/o carcinoma tongue	bilateral level IB, IIA, IIB & III	right level III	2.8 x 2.6 cm	1	1	1	1	1	1	0	1458.67	necrotic right level III with metastatic cells	squamous cell carcinoma of tongue with lymph node metastases to right level Ib and right level III with necrotic components and extracapsular extension	0	1
28	15676	41	M	c/o swellings in the neck and bilateral axillary region	level Ia, bilateral Ib, IIA, IIB, III, IV & V, VI, VII, VIII & X	left level Ib	2.5 x 2.4 cms	1	0	0	1	1	1	1	550.78	left level Ib node positive for lymphocytes cells	non- hodgkin lymphoma	1	1
29	14232	45	M	c/o swelling in the left lateral aspect of tongue	left level II and III	left level IIB	2.1 x 1.8 cms	0	0	0	1	1	1.1	1	1024.62	left level II shows malignant cells	squamous cell carcinoma of base of tongue with metastatic deposits to left level Ib, II and IV	0	1
30	13214	65	M	k/c/o carcinoma tongue with ulcerative growth	level IA, bilateral level IB, II and III	right level Ib	1.3 x 0.8 cms	0	0	0	0	0	1.6		989.28	NA	squamous cell carcinoma of tongue with no nodal metastases	1	0
31	15064	56	M	c/o fever with swelling in the left parotid region	bilateral level IB, II & III, left IVb and left VIII	left level II	1.9 x 1.9 cms	1	0	0	1	1	1	1	978.51	left level II node shows atypical cells	mucoepidermoid carcinoma of left parotid with metastases to left Ib, II and VIII	1	1
32	13587	76	M	c/o swelling in the tongue	bilateral level IB, II & III	right level II	1.2 x 0.7 cms	0	0	0	0	0	1.7	0	1009.47	NA	squamous cell carcinoma of tongue with no nodal metastases	0	0
33	14595	78	M	c/o growth in the tongue	level Ia, bilateral II,III, IV	right level II	2.4 x 1.1 cms	0	0	0	1	1	2.1	1	941.35	NA	squamous cell carcinoma of tongue with metastases to right level II nodes	1	1
34	12970	67	F	c/o ulcerative growth on tongue	bilateral Ia and Ib	right level II	1.8 x 1.2 cms.	0	0	0	0	1	1.5	0	1157.3	NA	squamous cell carcinoma of tongue with no metastasis to lymph nodes	0	0
35	13003	68	M	c/o lesion in the tongue	Bilateral level Ib & II	left level Ib	1.3 x 0.6 cms	0	0	0	0	0	2.1	0	1256.45	NA	squamous cell carcinoma of tongue with no metastasis to lymph nodes	0	0
36	9490	48	M	c/o lesion in the tongue	level Ia, bilateral level Ib, II and V	left level II	1.6 x 1.5 cms	0	0	0	1	1	1	1	978.45	NA	left level II and III show metastases	1	1
37	9865	40	M	k/c/o carcinoma tongue with ulcerative growth in floor of mouth	bilateral level Ib, II, left level III and IV	right level Ib	2.1 x 1.9 cms	1	0	0	1	1	1.1	1	998.08	right level Ib shows atypical cells	recurrence with metastases to bilateral Ib and left level II	1	1
38	15064	51	F	op/c/o right gingivo-buccal carcinoma with recurrence	right level Ib, II and bilateral VIII	left level VIII	3.0 x 2.4 cm	0	1	1	1	1	1.2	0	2723.74	malignant cells in the right level II lymph node	recurrence with nodal metastases to left level Ib, II and IV. Bilateral parotid lymph nodes show metastases with necrotic component	0	1
39	12469	57	M	c/o fever and swelling on right side of neck since 2 weeks	bilateral level II and III	left level II	1.4 x 0.5 cms	0	0	0	0	0	2.8	0	1254.45	reactive lymphadenitis	NA	0	0
40	15645	54	M	c/o hoarseness of voice	bilateral level II and III	right level II	1.4 x 0.7 cms	0	0	0	0	0	2	0	1213.34	NA	squamous cell carcinoma of glottis with no lymph nodal metastasis	0	0
41	16537	76	M	c/o ulcerative lesion in the tongue with right sided cervical lymphadenopathy	level Ia, bilateral level Ib, II, III and IVa	right level III	2.1 x 1.8 cms	1	1	1	1	1	1.1	1	1067.59	right level III lymph node positive for malignant cells	poorly differentiated squamous cell carcinoma of tongue with metastatic right level Ib, II and III lymph node with necrotic component and extracapsular extension	0	1
42	13087	67	M	c/o swelling in the left parotid region	bilateral level Ib and II	left level Ib	1.3 x 1.0 cms	0	0	0	0	1	1.3	0	1100.34	NA	mucoepidermoid carcinoma of left parotid gland with no metastases to lymph nodes	0	0
43	11649	35	F	c/o fever with cervical lymphadenopathy	level Ia, bilateral level II, III, IV & V	right level II	1.2 x 0.5 cms	0	0	0	0	0	2.4	0	1022.87	benign etiology- reactive lymphadenitis	NA	0	0
44	7311	71	F	c/o ulcerative lesion in the tongue	bilateral level IB, II and VIII	right level Ib	1.4 x 0.8 cms	0	0	0	0	0	1.7	1	1146.65	NA	squamous cell carcinoma of tongue with no nodal metastases	0	0
45	12025	65	M	op/c/o carcinoma tongue with swelling in the neck on right side	level Ia, bilateral level Ib, II and III	right level II	1.4 x 0.8 cms	0	0	0	0	0	1.7	1	1176.34	NA	squamous cell carcinoma of tongue with no nodal metastases	0	0
46	8436	51	M	K/c/o carcinoma of tongue with swelling in the neck on right side	level IA, bilateral level IB and II	right level II	2.2 x 1.4 cms	0	0	1	1	1	1.5	1	1463.54	necrotic right level II lymph node	carcinoma of tongue with metastatic right level Ib, II and III lymph node with necrotic component and extracapsular extension	0	1
47	7460	41	M	c/o ulcer on the tongue	level IA, bilateral level IB, II & III	right level II	1.6 x 1.1 cm	0	0	0	0	1	1.4	1	1023.46	NA	squamous cell carcinoma of tongue with no nodal metastasis	0	0
48	9578	50	M	op/c/o carcinoma of right parotid gland with recurrence	level Ia, bilateral level Ib, II and VIII	right level VIII	2.2 x 1.8 cms	1	1	0	1	1	1.2	1	1080.34	malignant cells in right level II lymph node	recurrence with metastases to right level II and VIII lymph nodes	0	1
49	8926	48	M	op/c/o carcinoma of tongue with swelling in the neck on left side	left level Ib, II, III, IV and V	left level II	1.8 x 0.9 cms	0	0	0	0	0	2	1	1067.98	left level II positive for atypical cells	no lymph nodal metastases	0	0